LUND
UNIVERSITY

The Quest for Excited States in ^{62}Ge

Emma Johansson

Master Thesis

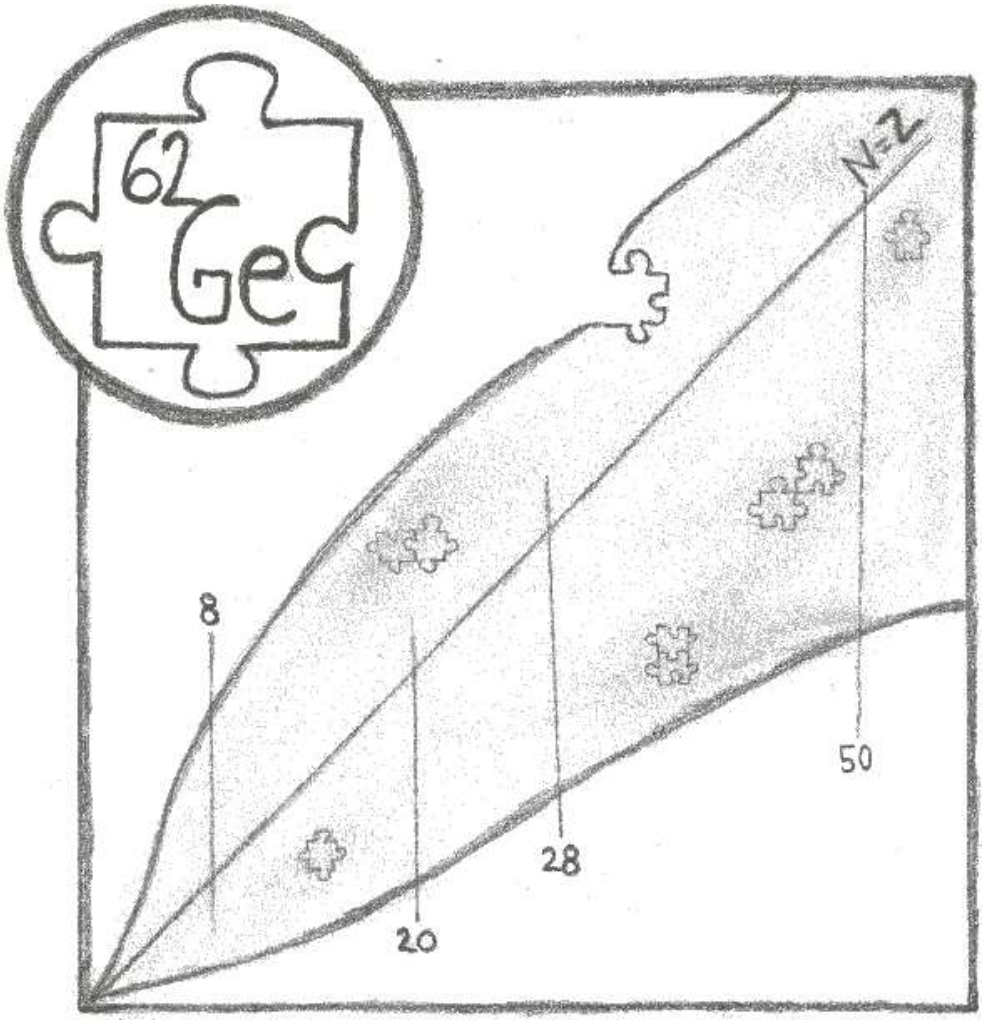

Department of Physics
Division of Nuclear Physics
LUNFD6/(NFFR-5023)/1-47/(2004)
Lund University
2004

Abstract

In an attempt to extend the knowledge of mirror nuclei into the mass region of $A = 60$, an experiment was conducted at the Holifield Radioactive Ion Beam Facility (HRIBF) at Oak Ridge National Laboratory in August 2003. The fusion-evaporation reaction ^{40}Ca + ^{24}Mg with a beam energy of 104 MeV was used to find previously unknown excited states in the $^{62}_{32}\mathrm{Ge}_{30}$ nucleus. The experimental setup comprised the germanium detector array CLARION, a recoil mass spectrometer and an ionization chamber. In the analysis of the data elaborate Doppler corrections routines have been developed using both the segmentation of the CLARION detectors and the total energy deposited in the ion chamber. Novel methods to obtain optimal Z-resolution have been probed. Despite low statistics, tentative evidence for the $4^+ \rightarrow 2^+ \rightarrow 0^+$ cascade in ^{62}Ge have been found. A large energy difference is seen in the 4^+ state in the ^{62}Ge-^{62}Zn mirror pair. This energy difference is most likely due to Coulomb monopole contributions, such as radial effects or electromagnetic spin-orbit interaction. A large scale shell-model calculation supports this preliminary interpretation.

Contents

Chapter 1

Introduction

Radioactivity was discovered by Henri Becquerel in 1896, but the atomic nucleus itself was not discovered until 1911 by Ernest Rutherford. This gave rise to a new field in physics, nuclear physics. Since then the study and applications of it has lead to such opposing uses as radiation therapy, nuclear magnetic resonance imaging, and weapons of mass destruction. No other field in physics has the potential for so much good or evil as nuclear physics.

The atomic nucleus is a many body system, consisting of strongly interacting fermions, protons and neutrons. Its properties are governed by the interplay between the strong, weak, and electromagnetic force. All nuclei can be given a position in a nuclear chart based on their number of neutrons, N and protons, Z. The light stable nuclei follow the line of stability, where $N \simeq Z$. Heavier nuclei tend to have more neutrons than protons, to damp out the increasing electrostatic repulsion between the protons, i.e to be stable. Nuclei on both sides of the line of stability exist, but they are unstable and they will decay towards the line of stability. The stability of a nucleus is related to its binding energy. The higher the binding energy the more stable is the nucleus.

The Nobel price in physics was awarded to Maria Goeppert-Mayer and Hans Jensen in 1963 for their shell-model of the nucleus. It is a mean field model, where every neutron and proton inside the nucleus experiences an average force due to all the other nucleons. This means that every nucleon occupies a defined state, which has a specific set of quantum numbers associated with it. Through experiments it was discovered that nuclei having certain numbers of protons and neutrons are more stable than their neighbors on the nuclidic chart. These are known as the 'magic numbers': 2, 8, 20, 28, 50, 82, and 126. This additional stability is a reminiscence of the unreactive noble gases where the electrons form closed shells. For nuclei far from the line of stability the magic numbers break down. Thus they are interesting to study, since they provide us with new information on how the forces act inside the nucleus as well as they test the limits of our theoretical models.

The lightest stable isotope of germanium is ^{70}Ge, and thus ^{62}Ge is far from stability. Until now only its bare existence has been proven, and its excited levels are completely unknown. The aim of this master thesis is to find and identify excited states of ^{62}Ge.

The mirror nucleus of ^{62}Ge is ^{62}Zn, their proton and neutron numbers are interchanged: $^{62}_{32}\mathrm{Ge}_{30}$ and $^{62}_{30}\mathrm{Zn}_{32}$. The nucleon-nucleon force seems to be nearly inde-

pendent of whether the nucleon is a proton or a neutron. This is called the charge independence of the strong force. Considering this, the differences in level energies of mirror nuclei should only depend on the Coulomb force. The Coulomb force of the nucleus depends on the spatial correlation of protons and its shape, and it changes with the energy and spin of the nucleus. The energy level difference of mirror nuclei is thus very sensitive to which configuration that forms an excited state, and by studying them the specific nucleons forming an excited state may be deduced. The excited states of ^{62}Zn are well known, and therefore it is of great interest to find the excited states of ^{62}Ge.

The experiment was conducted in August 2003 at the Holifield Radioactive Ion Beam Facility (HRIBF), at the Oak Ridge National Laboratory (ORNL), Tennessee, USA. ^{62}Ge was synthesized with a heavy-ion fusion-evaporation reaction, ^{40}Ca + ^{24}Mg, in which the excited ^{62}Ge is produced in the two neutron evaporation channel. By studying the subsequent γ-decay of ^{62}Ge, the excited levels may be deduced. ^{62}Ge is hard to produce since it has a very small cross section. It is estimated to be about 5 μb, which may be compared to the total reaction cross section of 120 mb. By having a low beam energy it is possible to enhance its relative cross section. From the cross section, it was estimated that 8 days of beam time would be enough to find the excited levels of ^{62}Ge. But we experienced some difficulties with the experimental equipment, among other things the ion source broke down twice. This resulted in the loss of almost half of the allocated beam time, which of course seriously reduced the amount of statistics collected during the experiment.

In this thesis the experimental method (Sec. 2.1) and the equipment used in the experiment will be described (Sec. 2.2). This is followed by a description of the data handling (Sec. 3) and the analysis (Sec. 4). A discussion on the results in comparison with theory and a shell model calculation is made in Sec. 5. Finally some conclusions are drawn and an outlook into the future is made (Sec 6).

Chapter 2

Experiment

The aim of this master thesis is to find excited states in the exotic nucleus ^{62}Ge. A fusion-evaporation reaction was initiated by letting a beam of ^{40}Ca hit a target of ^{24}Mg with an energy of 104 MeV, thus creating a compound nucleus of ^{64}Ge;

$^{40}\mathrm{Ca} + {}^{24}\mathrm{Mg} \rightarrow {}^{64}\mathrm{Ge}^*$

The compound nucleus is excited and decays first by evaporating particles. The residual nucleus of interest here,^{62}Ge, is created in the two neutron evaporation channel;

$^{64}\mathrm{Ge}^* \rightarrow {}^{62}\mathrm{Ge}^* + 2\mathrm{n}$

The ^{62}Ge nuclei are left in an excited state which decays by emitting γ-rays. These are the γ-rays we hope to detect in order to identify the excited levels of ^{62}Ge. In Sec. 2.1 I will describe the experimental method utilized in this experiment along with some basic theory on the fusion-evaporation reaction. Section 2.2 deals with the detection equipment.

2.1 Experimental Method

Incident beam nuclei and target nuclei can interact in many ways. For instance, there are transfer reactions, Coulomb excitation reactions, scattering, fusion, knock-out reactions etc. The type of reaction occurring between the beam and target nuclei depends on their relative energy and the centrality of the collision. In the same experimental setup many of these reactions may happen. The fusion- evaporation reaction is merely one possible interaction mode. It is the most probable for low energy, central collisions between medium weight nuclei.

The fusion-evaporation reaction may be thought of as a two step process. The incident beam nuclei hit the target nuclei. The individual nucleons of the beam and the target come into each others range of strong interaction, and the energy of the beam nuclei spreads throughout the whole system. The energy becomes shared between the nucleons, and a fused system is formed. Assuming the average kinetic energy of a nucleon is 20 MeV [1], one orbit around the nucleus takes $\sim 10^{-22}$ seconds. For the compound nucleus to be formed, the interaction of the beam nuclei with the target nuclei has to be much longer than 10^{-22} seconds. The compound nucleus is excited but the average energy of the nucleons is not large enough to free it from the nucleus. But through collisions between the nucleons some of them may gain enough energy to escape the compound nucleus. The compound nucleus is

thus an intermediate state existing after fusion but before decaying through particle evaporation. The compound nucleus 'forgets' the process of formation and decays by statistical rules [1], i.e the same compound nucleus can be formed in many different reactions. However, the decay probabilities depend only on the energy given to the system. The particle decay occurs within a time frame of $\leq 10^{-19}$ seconds [2]. Particle evaporation is an effective way of reducing the excitation energy in the

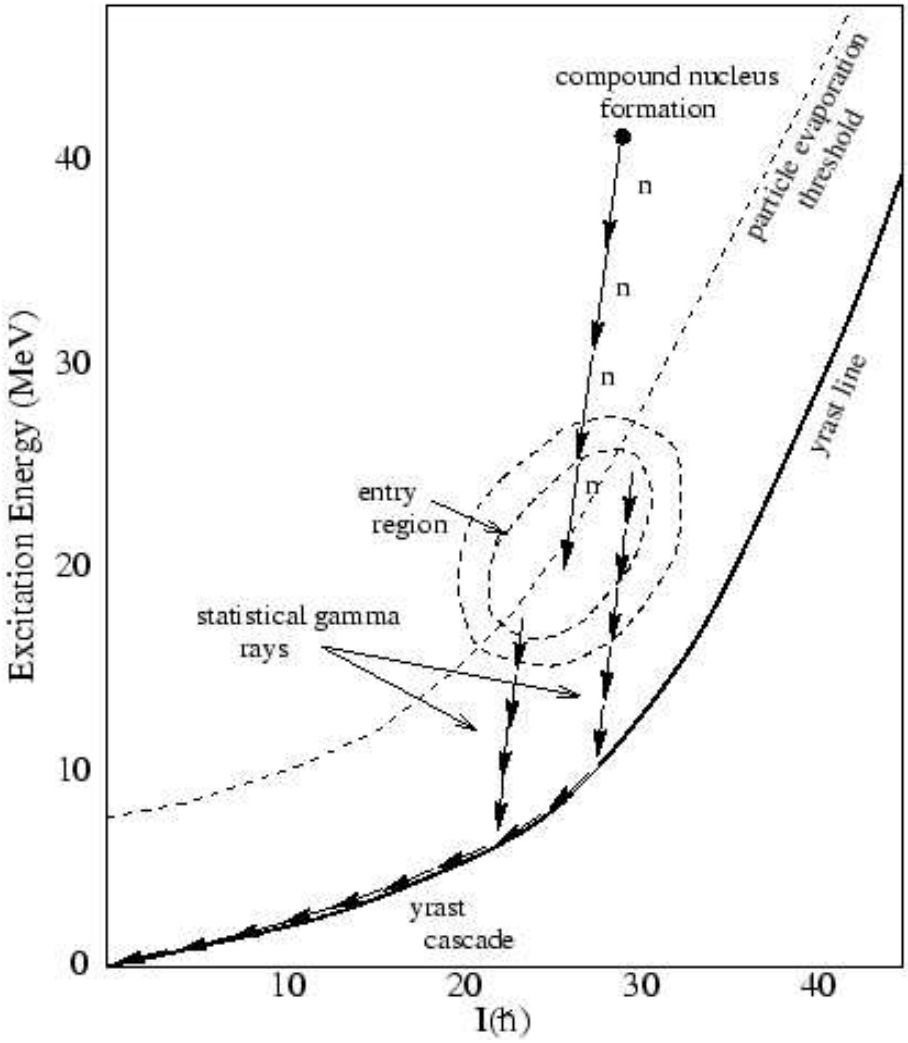

Figure 2.1: A schematic of the decay of a compound nucleus. Notice that it de-excites by particle evaporation followed by γ -ray emission to the ground state. The yrast line is defined as the line connecting the states with lowest possible energy for a given spin.

compound nucleus. For instance, an α-particle takes on average away $\sim$15 MeV and protons $\sim$5-6 MeV [2]. The more excited the compound nucleus is, the more particles are emitted. To optimize the neutron evaporation channel for our experiment the beam energy has to be large enough to form the compound nucleus (i.e, to overcome the Coulomb barrier), but small enough not to open up too many other decay channels. The optimum beam energy for the experiment is calculated in Sec. 2.1.1. The ^{64}Ge compound nucleus is proton rich, and by emitting protons it comes closer

to the desired line of stability. The proton excess causes the neutron separation energy to be much larger than the proton separation energy. This means that neutron evaporation is very rare in our experiment. For instance, in Fig. 4.2 in Sec. 4.1 the relative production of ^{62}Zn and ^{62}Ga nuclei can be seen. The two nuclei are produced from the same compound nucleus but in the two proton (2p) and one proton one neutron (1p1n) evaporation channels respectively;

$^{64}\mathrm{Ge}^* \rightarrow {}^{62}\mathrm{Zn}^* + 2\mathrm{p}$

$^{64}\mathrm{Ge}^* \rightarrow {}^{62}\mathrm{Ga}^* + \mathrm{n} + \mathrm{p}$

The production of the ^{62}Zn nucleus is *much* more probable than the production of the ^{62}Ga nucleus.

The average binding energy of the nucleons is about 8 MeV [1]. When the excitation energy of the compound nucleus is below $\sim$ 8 MeV, particle evaporation is thus no longer energetically possible. The nucleus then has to decay by emitting electromagnetic radiation, γ-rays. Notice that γ decay does not change the identity of the nucleus. The final product in the fusion-evaporation reactions is thus determined by the particle emission. The first γ-rays emitted from the very excited nucleus belong to transitions from the continuum , so called statistical γ-rays. As the nucleus continues to cool down, the discrete levels are reached and the γ-rays are then also discrete. These discrete γ-rays hold much information of the structure of the nucleus, and these are the ones of interest here. The γ-ray emission continues until the nucleus reaches its ground state. This is illustrated in Fig. 2.1 along with the particle evaporation threshold and the particle evaporation. The entire reaction, from formation of the compound nucleus to the ground state of the reaction product takes about 10^{-11}-10^{-9} seconds.

The beam of the present experiment consists as mentioned above of ^{40}Ca. It is formed from an ion source where the the calcium is in a molecular ion form, CaH^-. The CaH^- is extracted and ejected into a tandem accelerator. The tandem accelerator is an electrostatic accelerator which accelerates the ions by attracting them with a large positive potential, thus giving them energy. At HRIBF the tandem accelerator has a maximum potential of $V = 24$ MV. When the ions reach the terminal inside the accelerator, they hit a stripper foil which breaks the molecule and creates the ^{40}Ca with an average charge state of q=+6. The $^{40}\mathrm{Ca}^{+6}$ ions are then accelerated away from the terminal potential, thus producing the beam with the energy $E = (q + 1)V$.

The target was a 99.92% pure ^{24}Mg foil, which is 0.3 mg/cm^2 thin. The main contamination in the target is the ^{25}Mg isotope. The thickness of the target is chosen so the energy of the recoiling nuclei is rather well defined. The thicker the target, the broader energy distribution they have. The target is placed inside the target chamber, which can be seen in the middle of Fig. 2.4. Though the beam line and target chamber are in vacuum, the main contaminations in the target chamber are oxygen and carbon. The carbon comes from the cracked grease and oil used in the vacuum pumps. The oxygen arises from an oxide protection layer which the ^{24}Mg creates itself in air. The intensity of the beam hitting the target was on average 5 pnA (1 pnA = $6.3{*}10^9$ particles per second). The compound nucleus is then formed at a rate of $\sim$28000 nuclei per second. The target chamber itself is placed at the center of CLARION [3], which is a system of germanium detectors used to detect the γ-rays emitted by the recoiling nuclei, and which is described in Sec. 2.2.1.

The beam consist of ^{40}Ca is because it is the heaviest projectile available today having the same number of protons, Z, and neutrons, N. Using a heavy beam species and a lighter nucleus as the target is called a reaction in reverse kinematics. The advantage of reverse kinematics is, considering conservation of momentum, that the recoiling nuclei have a very distinct path of motion; along the beam axis in the forward direction. This means that a maximum number of recoils enter the Recoil Mass Spectrometer (RMS) giving us higher statistics in the experiment. The RMS [4] is the equipment used in HRIBF to separate the reaction products from each other and it is discussed in Sec. 2.2.2.

2.1.1 Calculation of the Beam Energy

The beam energy needed to optimize the production of ^{62}Ge at reasonable excitation energies was estimated, by studying other experiments where fusion evaporation has been used to investigate the 2n evaporation channel at or beyond the N=Z line. The experiments studied can be found in Refs. [5, 6, 7, 8]. From them some general features were gathered:

1. Each evaporated neutron is expected to carry away (on average) 1.5 MeV of excitation energy.

2. The excitation window for the 2n evaporation product was about 10 MeV.

This excitation window is chosen such as to minimize the available number of reaction channels. Next I considered which excitation level it would be preferable to reach in ^{62}Ge. The ground state of even-even nuclei such as ^{62}Ge has angular momentum and parity 0^+. The first two excited states are expected to be 2^+ and 4^+ at $\sim$1 MeV and $\sim$2 MeV excitation energy. Fig. 2.2 displays the energies of the reaction, the energy of the reaction window, the energy of the two evaporated neutrons, and the excitation energy of ^{62}Ge. Fig. 2.2 is used to approximate the excitation energy of the compound nucleus.
In the fusion-evaporation reaction the momentum has to be conserved:

$$p_b + p_t = p_{cn}$$

p_b (p_t) and p_{cn} are the momentum of the beam (target) and compound nucleus, respectively. The momentum of the target is zero. This gives:

$$p_b^2 = p_{cn}^2 <=> 2m_bE_b = 2m_{cn}E_{cn} =>$$

$$E_{cn} = \frac{m_b}{m_{cn}}E_b = \frac{A_b}{A_b + A_t}E_b \tag{2.1}$$

where E_{cn} is the kinetic energy of the compound nucleus, A_b (A_t) is the mass number of the beam (target), and E_b is the beam energy. The excitation energy expression of the compound nucleus is;

$$E_{cn}^* = E_b - E_{cn} + Q \tag{2.2}$$

Where the Q-value is the mass energy difference in the system, defined by

$$Q = (m_b + m_t - m_{cn})c^2,$$

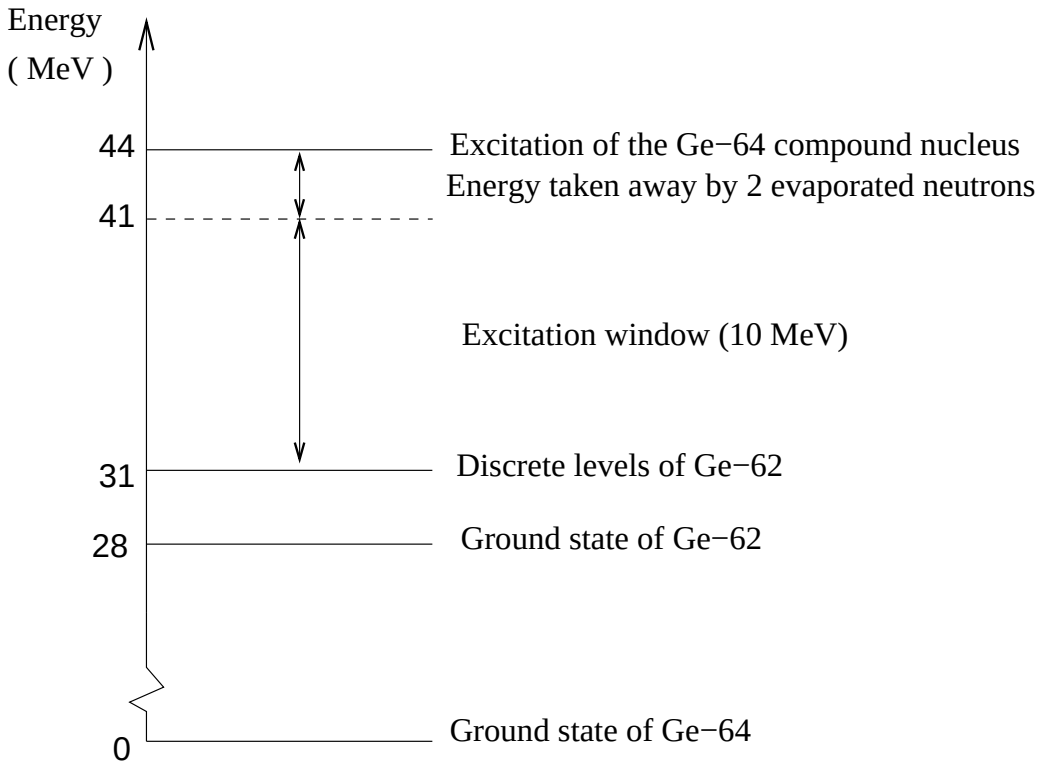

Figure 2.2: Sketch of how the excitation energy of the compound nucleus is approximated, to get the optimized beam energy.

where m_b (m_t;m_{cn}) is the mass of the beam (target;compound nucleus) and c is the speed of light. When Eqs. 2.1 and 2.2 are combined, the expression for the beam energy becomes:

$$E_b = \frac{E^*_{cn} - Q}{1 - \frac{A_b}{A_b + A_t}} \tag{2.3}$$

Where E^*_{cn} is taken from Fig. 2.2 and A_b, A_t and the Q-value are as above. This yields a a beam energy of E_b∼104 MeV, which is the energy used in the experiment.

2.2 Detection equipment

2.2.1 CLARION

At HRIBF the detection system designed to detect γ-rays is the CLover Array for Radioactive ION beams (CLARION [3]). It is an array consisting of 44 germanium crystals arranged around the target chamber. The germanium crystals are semiconductor detectors. The reason why the array consists of germanium crystals is their superior energy resolution. The germanium atom has four valence electrons, which form covalent bonds to electrons belonging to a neighboring atom. The germanium crystal has a band structure where the valence band is full, and thus the conduction band is empty. The energy gap between the bands is about 1 eV. At

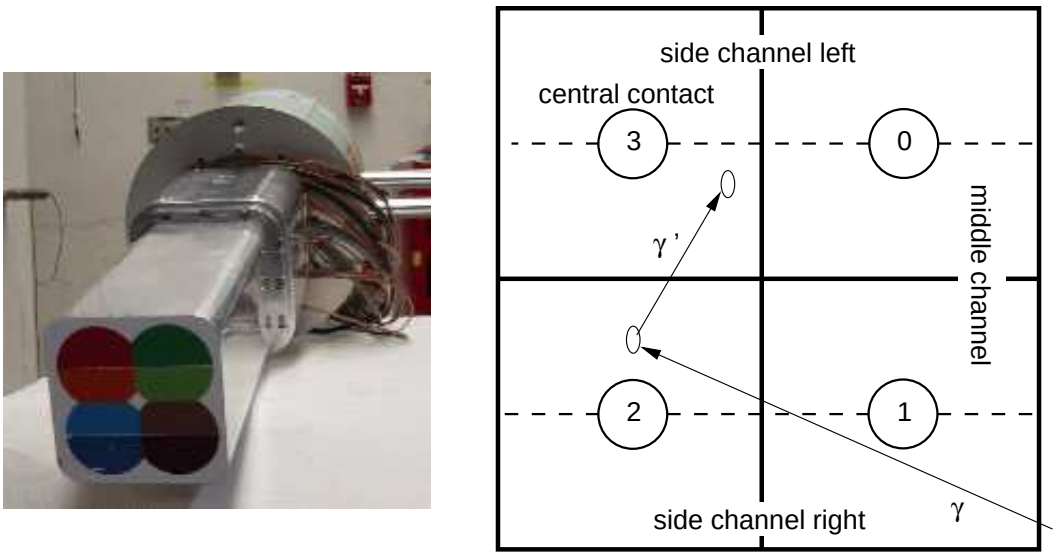

Figure 2.3: A photograph of a clover and an image of a clover with its segmentation. The clover consists of four germanium crystals which are segmented into three side channels. Notice that the segmentation makes it possible to detect up to seven signals from each clover. The seven possible signals are very important when the reconstruction of the γ-ray energy is performed.

room temperature electrons can be thermally excited across the gap. When the germanium crystals are used for γ-ray detection, they are cooled to 77 K in order to avoid this thermal excitation as much as possible. The germanium material is of high purity, HPGe, the level of contaminants in the crystals are typically 10^9 atoms per cm^3 [9], which is a very low level of contaminants. Even so, the contaminants cause the crystals to be mildly p-doped or n-doped, depending on the contaminants present. By applying a small amount of the opposite dopant onto one side of the crystal, a flow of holes from the p-doped material and a flow of electrons from the n-doped material creates a region with no net charge. This is the depletion region. The crystal is then placed in an electrical circuit with reverse bias and it works as a large p-n junction diode. When the γ-ray interacts with the crystal, electron-hole pairs are liberated from the crystal. In the presence of the electrical field they will start to migrate. The more energy the γ-ray deposited, the bigger the current. The signals coming from the crystals can be turned into information on the incident radiation, i.e, can be turned into spectra. More on how the signals are handled can be found in Sec. 3.1. In Fig. 2.3 the central contacts are marked. This is one of the connections of the crystal in the circuit. The energy needed to create one electron-hole pair is about 3 eV [9], so a 1 MeV γ-ray will give rise to more than a hundred thousand information carriers. This is why a germanium crystal has such a good energy resolution.

The crystals are placed into groups of four, which is called a clover detector. CLARION has 11 clovers detectors. Ten of the clovers are segmented into three channels, which are indicated in Fig. 2.3, giving the possibility to detect up to seven signals from each clover detector. The combination of four crystals allows for *add-back* which can improve the efficiency of the clover. The physical motivation for doing

add-back is the way γ-rays interact with matter.
A γ-ray can interact with matter in three different ways. Through Compton scattering, photoelectric absorption, and with pair production. I will just give a very short general reminder of the way they work. In Compton scattering the γ-ray scatters from an outer shell electron in the crystal with an angle θ, thus giving some of its energy to the electron. The γ-ray will after scattering move on, in a different direction and with a lower energy, (see Fig. 2.3). Photoelectric absorption occurs when the γ-ray is completely absorbed by the crystal material (in Fig. 2.3 this means that no γ' would be present.) The ejected electron leaves a hole in the structure of the crystal. This hole is quickly filled by other electrons, giving rise to X-rays. These X-rays are also absorbed by the crystal. The energy of the ejected electron is also absorbed and the reaction can repeat itself many times until all the energy of the original γ-ray is deposited. The third process for the γ-ray to interact with matter is with pair production. Pair production is the main process when the γ-ray energy $\simeq$5 MeV. Thus in our experiment pair production is not an important process.
The way a γ-ray interacts with matter depends on the energy of the γ-ray and the atomic number, Z, of the matter it interacts with (or rather the number of electrons present which is equal to Z). For the crystals consisting of germanium (Z=32), the photoelectric absorption dominates up to $E_\gamma\sim$200 keV. For energies larger than $\sim$200 keV compton scattering dominates [9].
Add-back can be explained with the help of Fig. 2.3. A γ-ray enters crystal 2 and then compton scatters into crystal 3. In crystal 3 the γ-ray interacts via photoelectric absorption. This γ-ray is detected as two separate γ-rays, but none of the 'two γ-rays' have the true energy of the incident γ-ray. This contributes to the background in the spectra. It also means that statistics in the full energy γ-ray peak is lost. With add-back will the 'two γ-rays' be understood as one γ-ray and its energy can be reconstructed with the correct energy, which will be discussed further in Sec. 3.2.2. The crystal to crystal distance is 2 mm. Minimization of the dead layer between the crystals is important in order to do good add-back.
The γ-ray can also scatter out of the clover. This also increases the background level of the spectra, since the γ-ray did not deposit its full energy. The clovers have an *anti-compton shield* surrounding it. The clover and the shield work in anti-coincidence, which means that if a γ-ray is scattered out of the clover and hits the shield the event is rejected. The shield is mainly made of bismuth germanate (BGO). BGO has good timing properties, which is useful when anti-coincidence is used. Secondly BGO has a large density (7.1g/cm^3 [9]) which means that a scattered γ from the clovers, will most likely be stopped in the BGO. Also the high Z of the bismuth increases the probability for the scattered γ-ray to interact with it. The high density of BGO also means that the shielding can be relatively thin, which is necessary, when the clovers are placed into an array.
With the add-back the detection efficiency of a clover detector in CLARION is 150% relative to a 3"x 3" standard NaI detector [3]. The total photo peak efficency gives a measure of the arrays power to collect the γ-rays energy, for CLARION it is 2.6% for an energy of E$_\gamma$=1.3 MeV [3], which is an average efficiency compared to other contemporary arrays. The clovers can be placed at three different distances (20.0, 21.7, and 23.5 cm) from the target. In Fig. 2.5 one of the clovers is being moved, between two of these distances. The majority of the clovers are placed in

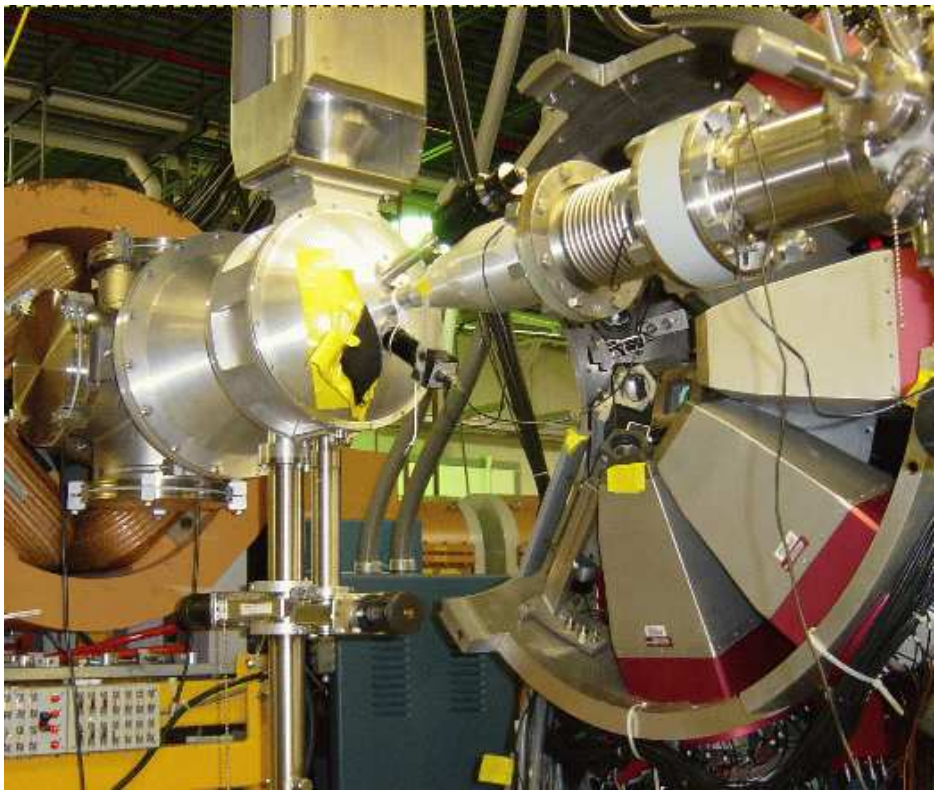

Figure 2.4: One half of the open CLARION. The beam line is coming form the right, and in the middle the target chamber is visible. When the CLARION is operational, the two symmetrical halves are closed. Do notice the clovers, which can be seen in a close up in figure 2.3. Here the clovers are coated by BGO-shields. On the left hand side is the first part of the RMS is visible.

the backend part of the sphere, with angles varying between 90° to 160°. The sphere can be opened and in Fig. 2.4 one half of the CLARION is visible. This leaves room in the forward part of the sphere for, e.g., particle detectors. It is also strategic to keep the the clovers away from the forward direction, since the flux of particles is the highest in that direction and the clovers are sensitive to radiation damage.

2.2.2 Recoil Mass Spectrometer and Ion Chamber

How do we know which γ-ray belongs to which nucleus for the 28000 nuclei produced every second which de-excite by some 15 γ-decays each? There is obviously a need to distinguish between the reaction products. This is done by using a Recoil Mass Spectrometer (RMS) and an ion chamber (IC). A RMS consist of several magnets and electrical fields designed to separate the different masses. In Fig. 2.5 the RMS at HRIBF can be seen where 7 quadropules (Q1-Q7), two sextupoles (S1,S2), three magnetic dipoles (D1-D3), and two electrostatic dipoles (ED1,ED2) are marked. The RMS has an angular acceptance of $\pm$30 mrad in the horizontal direction, and $\pm$110 mrad in the vertical direction [4], again stressing the point of reverse kinematics. The first quadrupole (Q1) can also be seen in the left part of Fig. 2.4. The first

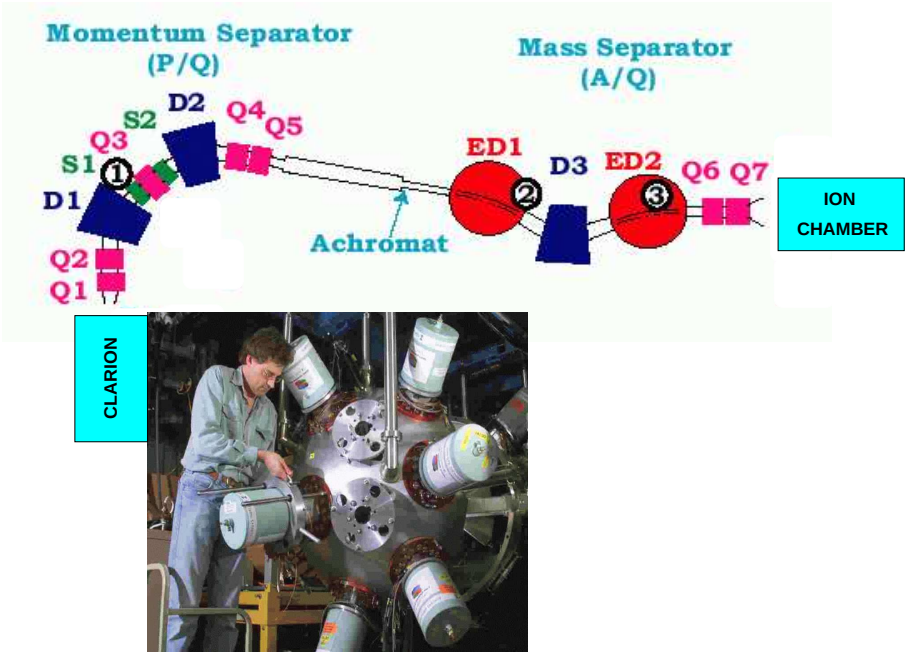

Figure 2.5: A schematic of the experimental equipment with the relative position of the recoil mass spectrometer, the ion chamber, and CLARION. The different magnets and electrical fields of the RMS are marked. Specifically, there are 7 quadropoles (Q1-Q7), two sextupoles (S1,S2), three magnetic dipoles (D1-D3) and two electrostatic dipoles (ED1,ED2).

part of the RMS separates the recoils by their momentum. The primary aim of this is to minimize the presence of beam in the remaining part of the RMS. The recoils are then refocused at the achromatic focus. The second part of the RMS separates them by their A/Q-ratio. The mass-to-charge ratio means that a specific mass with a certain charge state can be selected to enter the IC. The RMS is set so that $A = 62$ with $Q = 18.10$ enters to the right side of the detector.
The ion chamber is filled with gas. When the recoiling nuclei enter it, they will interact with the gas and thus loose energy. Even though the nuclei may enter at the same point in the IC with the same A/Q ratio, they can still have different Z; for instance, ^{62}Ga and ^{62}Zn. They have the same mass, but they have different proton numbers. This means that they will loose energy in different ways, which makes it possible to detect which one of these nuclei is present in the IC. The IC is divided into three parts, and for each part the energy loss can be detected. This is very important in the identification process, which will be discuss in Sec. 4.1. A more detailed description of that part of the experiment and analysis can be found in the Master thesis by Lise-Lotte Andersson [10].

Chapter 3

Data Handling

3.1 Data Acquisition

The signals coming from the CLARION and the ion chamber have to be combined, in order to know which nuclei emitted which γ-rays. This is done by enforcing some criteria on the signals. Figure 3.1 is a rough block diagram of the electronics associated with the CLARION and the IC. The diagram is willingly a very schematic representation of the real electronics.

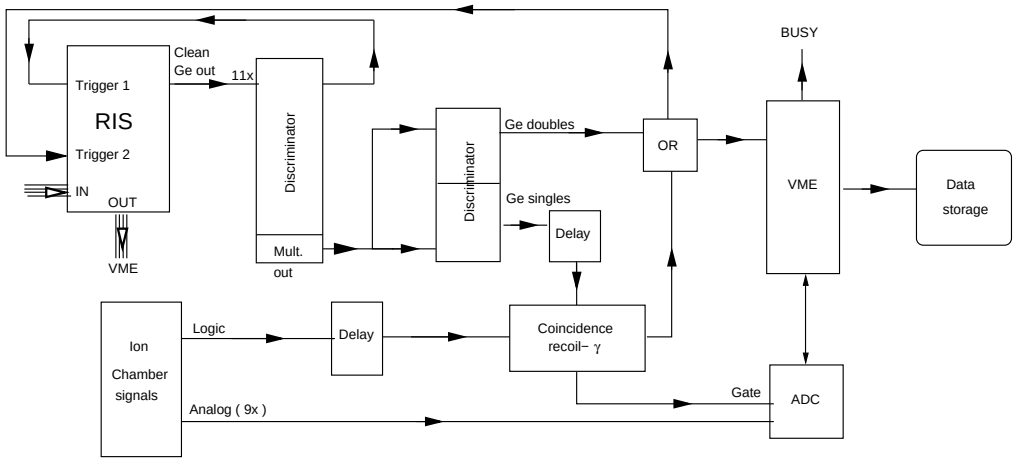

Figure 3.1: A simplified block diagram of the CLARION array and the ion chamber electronics.

The RIS module can handle information from multiple sources. It can also redirect the information to many destinations. Each RIS module handles all signals from the segmented clover crystals and its surrounding BGO suppression shield. It first checks if the Ge signals are clean, i.e no anti-coincidence signal from the BGO has come. If so, the signal passes on to the discriminator. The signal has to be of a certain length, height and shape. If the signal is valid, the discriminator passes the signal on. Then trigger 1 tells the RIS module to get ready for further processing, e.g, analog to digital conversion of the Ge energies and times. Depending on whether the multiplicity of all the RIS modules corresponds to a single hit in the CLARION (one γ) or to two hits (two γ's), the signal 'ge singles' or 'ge doubles' is generated. If it is a double hit, the signal triggers trigger 2, and the data read out can start via

the VME module. If the VME was already busy, the new trigger will be ignored. The data is then stored in a list-mode file on the computer.
If it was a single hit, the corresponding signal enters a delay. The γ decay occurs within a time frame of $\leq 10^{-9}$ seconds, after which the recoil is moving through the RMS and into the IC. This takes $\sim 10^{-6}$ seconds. Thus γ-ray signals have to be delayed so that the IC signal can be processed. The system waits for the recoil to give a signal in the IC. If the proper IC signals come, the VME is set off again, and the data is collected.
In the data stream the events come one after each other, i.e, on an event-by-event basis. We separate the data stream into so called runs. This is done by stopping and starting the data collection on the data acquisition computer. The runs are chosen such that every data set is reasonably sized ($\leq$ 1 GB), covering not too long time periods ($\leq$ 8 hours), and taking into account changes of the experimental settings. This helps with the re-calibrations, as the clovers can change their response during the experiment, as well as the RMS and the IC can drift slightly from the nominal values. Finally the data was burned onto DVD and brought to Lund for off line sorting.
To sort the data a program package called `tscan` was used. In the first section of the program, the raw data is read event by event. Each parameter of the experiment, e.g energy, time etc. is defined by an identification number and its data value. First of all, consistency checks are performed, e.g the time and energy signals for a given germanium crystal or all four signals from one side of the IC must be present. In the next section of the program, the parameters are calibrated and corrected for drifts, the clover signals are handled with add-back (see Sec. 3.2.2) and a detailed Doppler correction (see Sec. 3.2.3) is performed. Finally, the signals from the IC are handled to identify the A and Z of the recoiling nuclei (see Sec. 3.3 and [10]).

3.2 Calibration of the Germanium Detectors

3.2.1 Energy and Time alignment

The germanium crystals have to be calibrated in energy, since they do not have a linear response to the deposited energy. Different crystals may also differ in their response to the same incident γ-ray energy. To calibrate them radioactive sources with known γ-ray transitions were used: ^{152}Eu,^{133}Ba, and ^{88}Y. These were chosen because they have peaks at well known energies, and span the energy region of interest very well. The uncalibrated peaks were connected with their true energy, and with the help of a program called `encal` [11], the 44 crystals were gain matched with second degree polynomial functions. The crystals were also aligned in time. In Fig. 3.2 the time signal versus the trigger 2, (which may be seen in Fig. 3.1) from one crystal is shown. In the figure I have marked the area in which the time is defined as being a $\gamma\gamma$ event or when it is considered to be a recoil-γ event. This means that if an event occurs within a certain time interval, it is known whether it is a $\gamma\gamma$ event or a recoil-γ event. The windows are chosen by the settings in the delay electronics above. The windows allow a reduction in the background level, since an event, that does not belong to the time interval, of for instance, a recoil-γ event, can be disregarded.

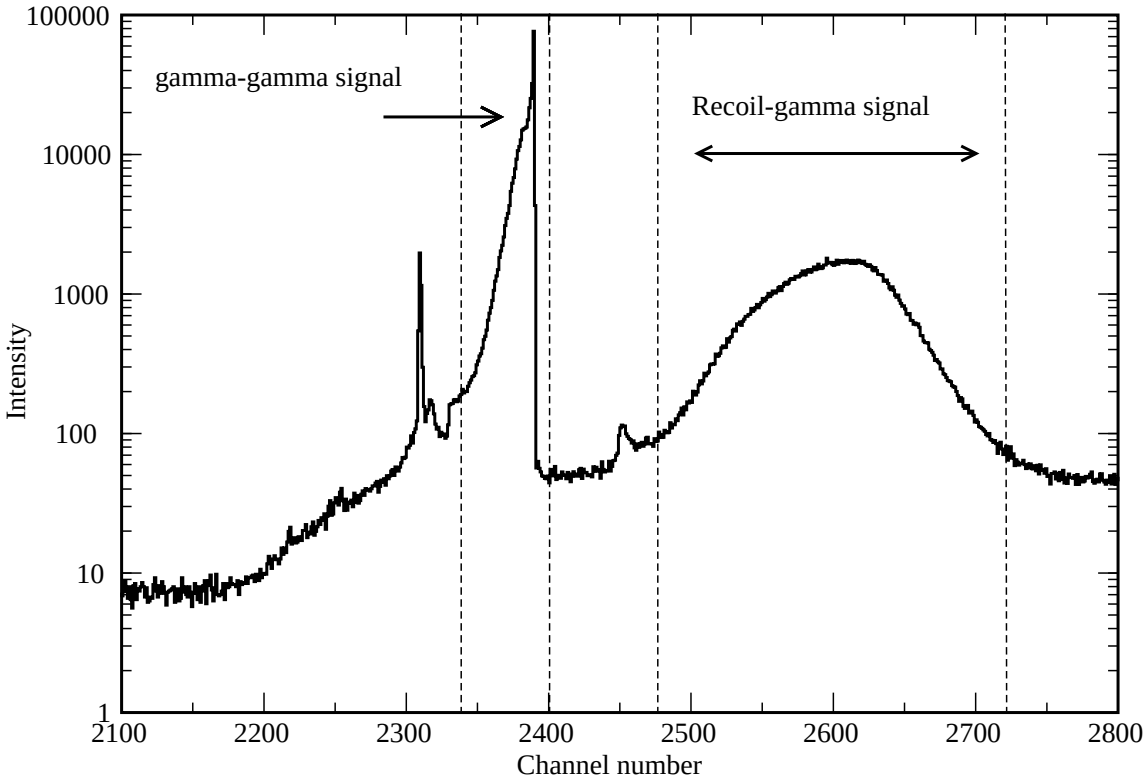

Figure 3.2: A time spectrum of a germanium crystal versus the trigger2, including the the time windows for different event types.

3.2.2 Add-Back Method

As was mentioned in Sec. 2.2.1 the add-back method allows for the γ-ray energy to be reconstructed, so its true energy is determined. The first thing I had to decide was: When is it possible to do add-back and when is it not? If a γ-ray enters the crystal and then scatters into another, two signals are registered, and to be able to reconstruct the energy of the γ-ray the two signals have to be added together. But how can this be separated from an event where two independent γ-rays entered the clover at the same time. In order for the two γ-rays to be considered as entering the clover at the same time, they have to be detected within a time range of $\sim$30 ns from each other. If the two independent γ-rays are added together, a false summation peak is created. Needless to say, this is not desired. When the individual energy deposited by two or more γ-rays in the clover is larger than the add-back threshold, the energy of them is summed together. In Fig. 3.3 the effect of two different add-back thresholds is indicated, a false peak has been created. The true peaks were generated by the 'ge single' hits in the clover, from them a spectra was produced. In the 'ge double' hit spectra, the false peaks can be created with a high add-back threshold. Through comparing the intensity of the false peaks and the real peaks, for different add-back thresholds the optimum threshold was determined to be 20 keV. At this level, the false peaks were no more than 2% of the real peaks but the statistics increased by 25% for a γ-ray energy of 1 MeV. In Fig. 3.4 the effect of the

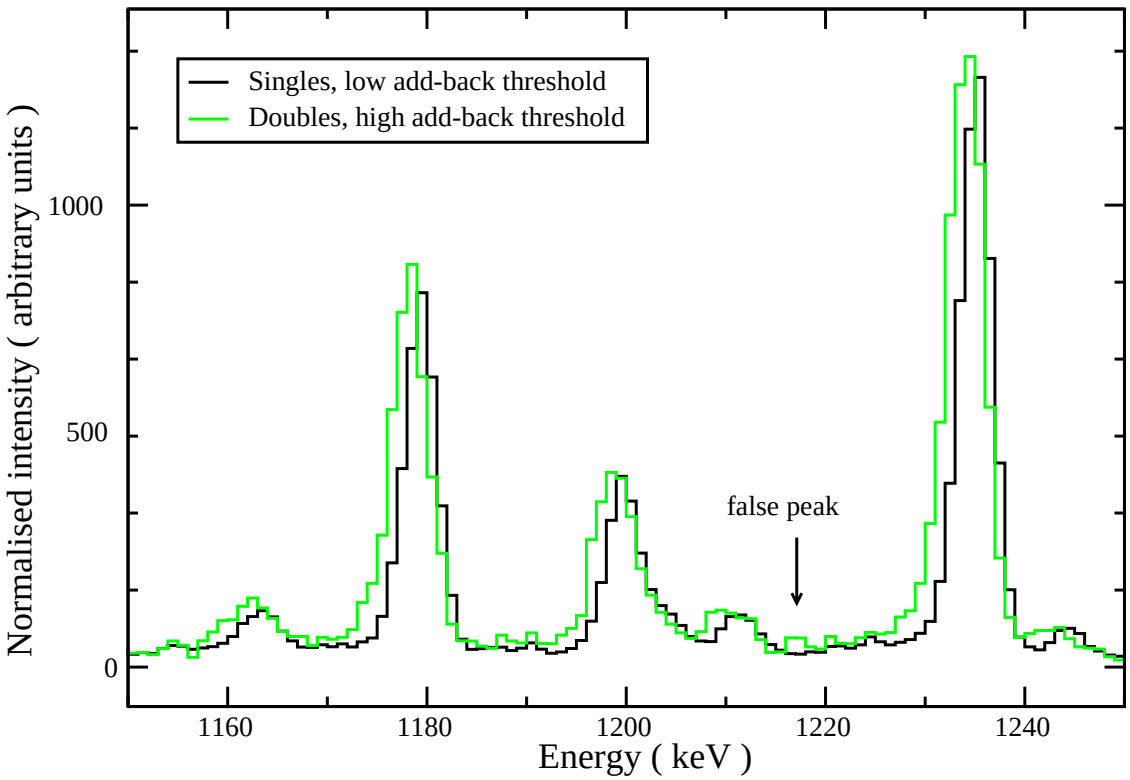

Figure 3.3: An $A = 62$ spectrum, the black curve describes when the clover has been hit by a single γ-ray, with a low add-back threshold (20 keV). The green curve describes when the clover has had two hits in it, with a high threshold (200 keV). The two hits can be two independent γ-rays or it can be one scattered γ-ray. The created false peak is visible in the green curve.

add-back mode can bee seen.

The advantage of add-back is a reduction of the background level in the spectra, as well as the increased statistics. With the add-back level fixed, an **e**fficiency calibration was performed. The efficiency of a germanium crystal is not linear in its response to γ-ray energy. For this setup they are the most efficient for a γ-ray energy of about 300 which can be seen in Fig. 3.5. The clovers were grouped into three rings for the efficiency calibration, at 96°, 131°, and 154° with respect to the beam axis. The benefit of making the rings is the increased statistics. A program called `effit` [11] was used to fit an efficiency curve to the measured intensities of γ-ray peaks for the calibration sources mentioned above. Some of the data points may actually harm the fit more than they help it. In the calculated efficiency curve Fig. 3.5 the 2.7 MeV γ-ray energy of ^{88}Y was removed, since it also has a contribution from a summation peak. Fig. 3.5 shows the calculated efficiency curve for all the rings. The dots corresponds to the efficiency of the calibration sources. The effect of add-back is more prominent for energies above $\simeq$1 MeV. If the add-back mode had not been used, the efficiency in this energy region would be much lower, than it is in Fig. 3.5. We also investigated the triple and quadruple hits (when three or all four crystals) have events in them. The statistics for these events was very small,

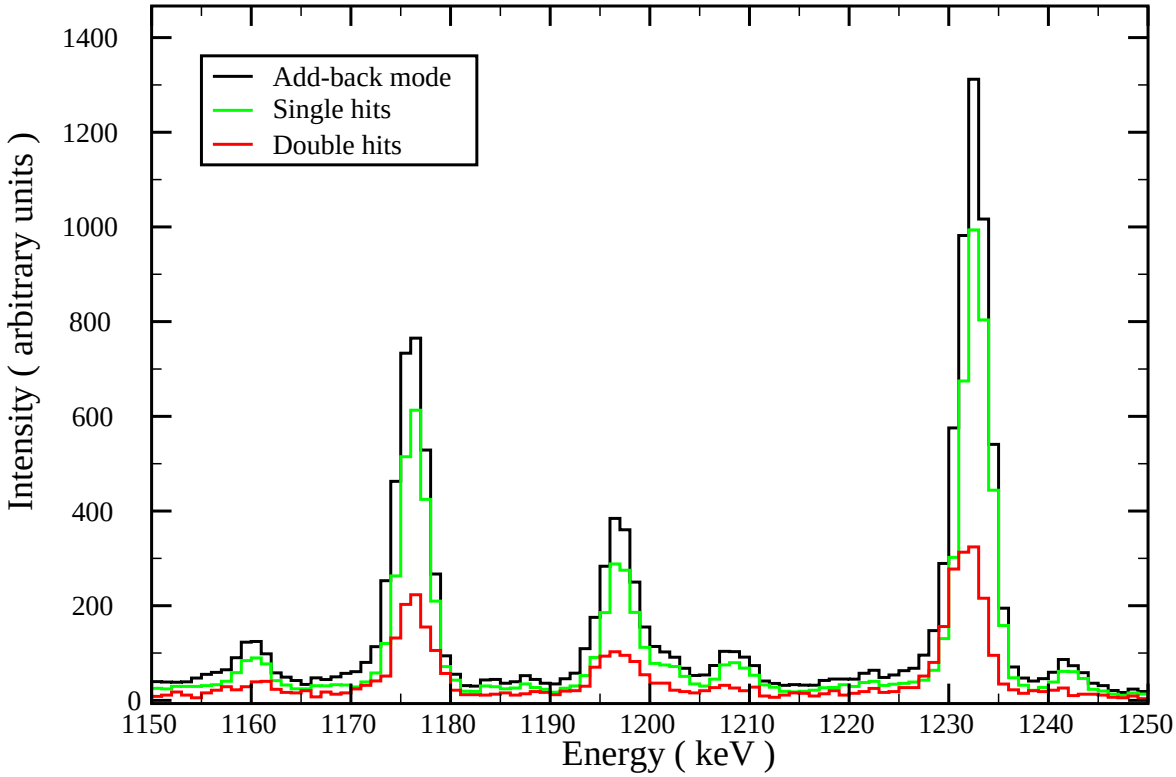

Figure 3.4: The effect of add-back mode for a clover placed at 160°. The green (red) curve represents single hits (double hits) in the clover. The back curve shows the sum of them. An $A = 62$ spectrum.

only ∼3% of the single hits, and their FWHM was large. It was therefore decided to not include them in the final sorting.

3.2.3 Doppler Corrections

The calibrations and alignments above were made with γ-rays from the calibration sources. One major difference between these and the 'real' data is that the recoiling nuclei are moving, causing their emitted γ-ray energy to be Doppler shifted according to:

$$E_\gamma = E_{\gamma_0}(1 + \frac{v}{c}\cos\theta) \tag{3.1}$$

E_γ is the measured energy of the γ-ray, E_{γ_0} is the true energy of the γ-ray, v is the velocity of the recoils, c is the speed of light, and θ is the angle of the crystal. To get the true energy of the emitted γ-ray, the Doppler effect has to be corrected for. Three corrections were performed, an average velocity correction, a nominal angle correction, and an individual velocity correction. The corrections were made on mass gated spectra this means that only the γ-rays from the desired $A = 62$ mass are considered.

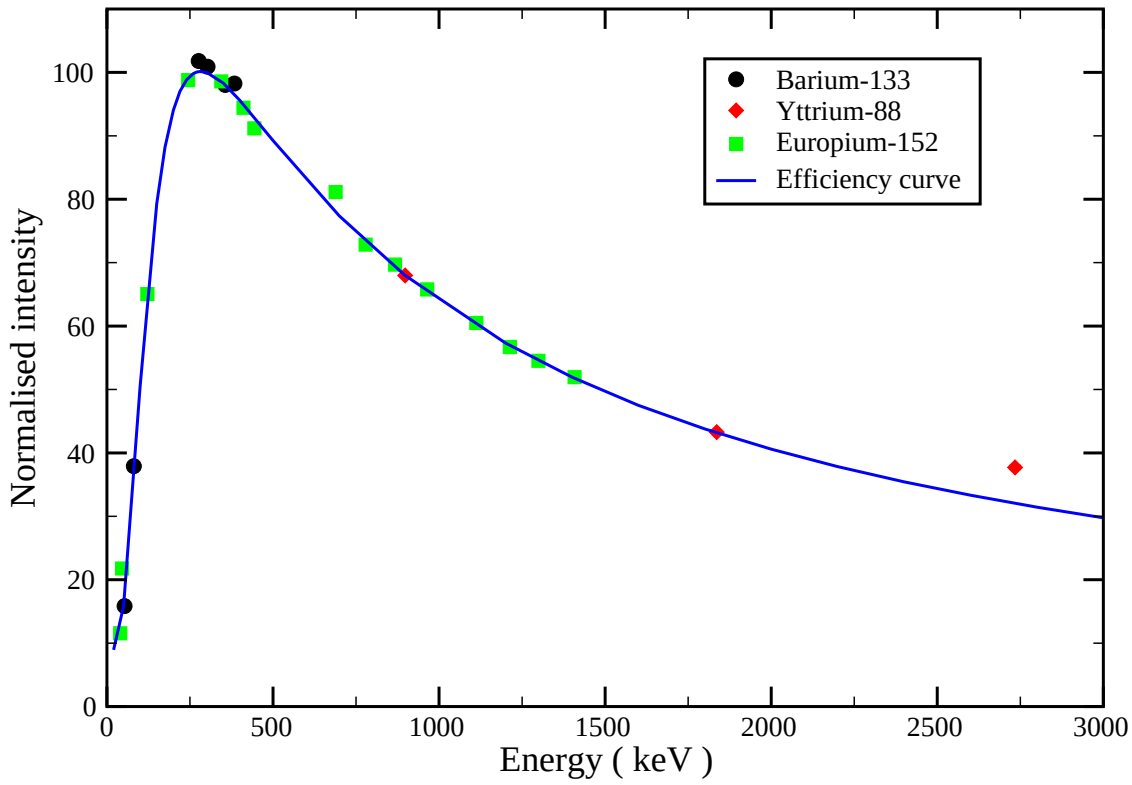

Figure 3.5: The efficiency curve for all the rings, as well as the experimental points.

- **Average velocity correction**

  When looking at Eq. 3.1 the only truly unknown value is the velocity of the recoiling nuclei. The average velocity of the recoiling nuclei can be calculated with the help of Eq. 3.2. For a known nucleus, for instance ^{62}Zn, the true γ-ray energy is known, the angle of the crystal detecting the γ-ray is known, and the measured energy is known. The energy of one low energy peak E_{γ_l} and one high energy peak E_{γ_h} was measured in each of the spectra from the 44 crystals. From this an average velocity can be calculated.

$$\frac{v}{c} = \frac{\frac{\Delta E_\gamma}{\Delta E_{\gamma_0}} - 1}{cos\theta} \tag{3.2}$$

  where $\Delta = E_{\gamma_h} - E_{\gamma_l}$, for both the measured energy values and the tabulated values. The average velocity of the recoils turned out to be 4.26% of the speed of light. This velocity and an equation were programmed into the `tscan` program, in such a way that every crystal is corrected in accordance with the angle it is positioned in. In Fig. 3.6 this first correction may bee seen for a crystal placed at 160°, along with the other corrections made. The effect of the first correction is more dramatic for the crystals placed at larger angles since;

$$\theta \rightarrow 180^\circ \Rightarrow \cos\theta \rightarrow -1,$$

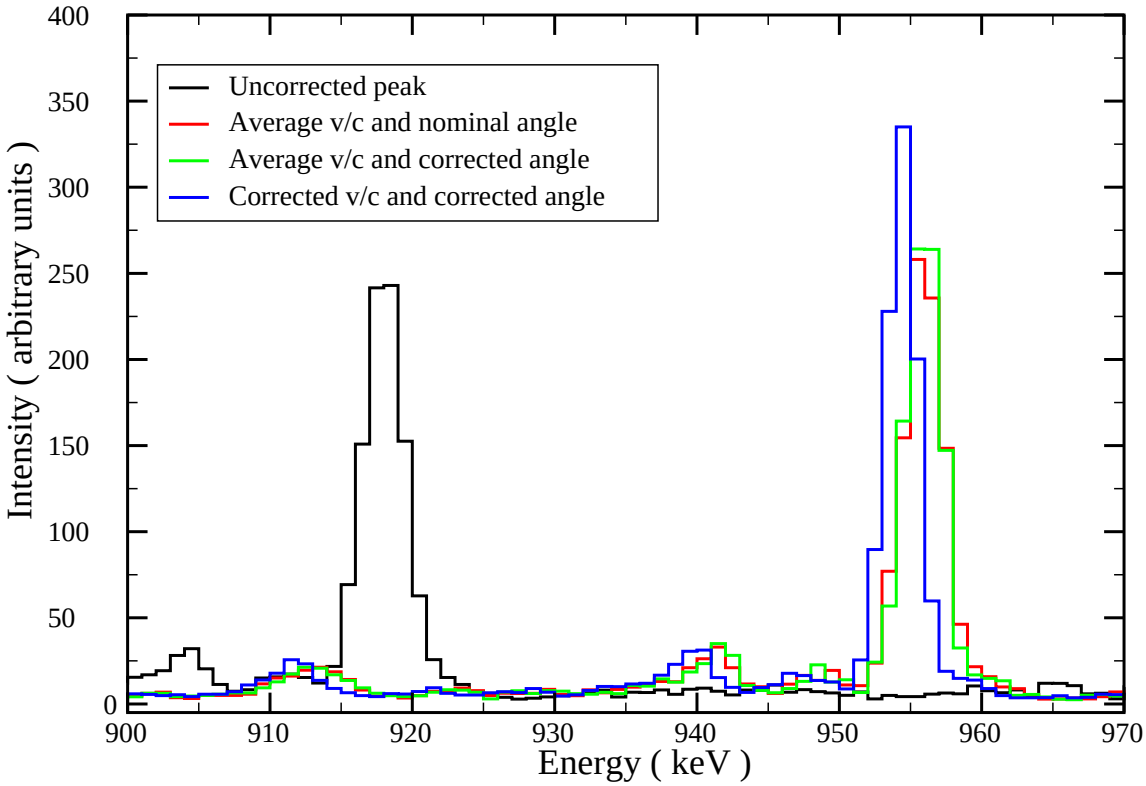

Figure 3.6: Spectra of the different stages of the Doppler corrections for a detector placed at 160°.

whereas for the crystals closer to 90° the effect is more subtle, because:

$$\theta \rightarrow 90^\circ \Rightarrow \cos\theta \rightarrow 0$$

For comparison, check Fig. 3.8 where this first correction is also marked for a crystal placed at 84°.

- **Angular correction**

  The crystals are a few centimeters wide. Thus the angle that is given, the nominal angle, is an average angle, which is in principle true only for the center of the crystal. But not all the γ-rays will hit the detector in the exact middle of it. There is a need to find an effective angle for a given γ-ray for the crystals as well as for the full clover in case of add-back. First I will describe how the effective angle for the crystals was found. The crystals are segmented into two parts, a side channel and a middle channel which may be seen in Fig. 2.3. This can allow for a finer determination of the angle of the detected γ-ray. The first thing to decide is which side of the crystal the γ-ray entered. In order to know this, the way the crystals are physically placed in the clover has to be known. This may seem trivial, but it is not certain that a clover connected as left-middle-right channels is in reality placed so. The clover might have been moved and then put back as right-middle-left, in which case the γ-ray is interpreted as entering from the opposite direction. We

looked at the signals from every crystal to see if it had a 'left' or 'right' signal. Then we reprogrammed the program to fit the actual position of the crystals in the clover. It turned out that almost half of the clovers were placed in the opposite way than they were supposed to.

To know which side of the crystal the γ-ray hits first, it is assumed that the γ-ray deposits most of its energy in the first interaction with the crystal due to the probability distribution of the Klein-Nishina Compton scattering formula. The first task is to select cases when the γ-ray enters the side channel or the middle channel. This was done by looking at the parameters:

$$y = 100\frac{E_m}{E_c} \tag{3.3}$$

E_m is the energy deposited in the middle channel of the crystal, and E_c is the energy deposited in the entire crystal. This parameter is plotted as a function of the total energy in the crystal in Fig. 3.7. Consider when the γ-ray enters the middle channel, and there deposits its full energy. The energy deposited in the middle channel and in the entire crystal is the same. The y-parameter is then 100. The extreme opposite of this is when the γ-ray deposits its full energy in the side channel. In that case the energy in the middle channel is zero corresponding to a position in the bottom of the matrix. In between these extremes are the cases when the γ-ray enters in one part, and then scatters into the other part. By putting a gate along the y-axis and projecting out, the γ-ray spectra of the different cases can be studied. In Fig. 3.7 the gate can be seen. It corresponds to all the energy being deposited in the middle channel of the crystal. In Fig. 3.9 two peaks from the projected γ-ray spectra can be seen. The slight difference in the position of the peaks, gives rise to the corrected angle. By using Eq. 3.4 the corrected angle can be calculated.

$$\theta = \arccos(\frac{c}{v}(\frac{E_\gamma}{E_{\gamma 0}} - 1)) \tag{3.4}$$

From this a function for the corrected angle as a function of y is derived. This means that for every event we get an effective angle. For instance, a detector placed at 84° will now have an angular range of 84°±2.6°. The effect of this correction can be seen in both Figs. 3.6 and 3.8. In Fig. 3.8 the effect of the angle corrections can be seen; the peak becomes more narrow, and thus the FWHM is improved. This stems from the fact that the Doppler broadening is most pronounced for crystals at 90° because:

$$|\frac{dE_\gamma}{d\theta}| = E_{\gamma 0}\frac{v}{c}\sin\theta d\theta \tag{3.5}$$

The basic method for angle correction for double hits is the same as for single hits. It is somewhat more complicated, since there are more options on how the γ-ray can enter and scatter in the clover. If the γ-ray scatters 'vertically' in the clover, it is the same case as above as the angular range does not change in the 'vertical' direction. The horizontal angle correction, which we did and programmed is a very important feature in the program. The vertical and

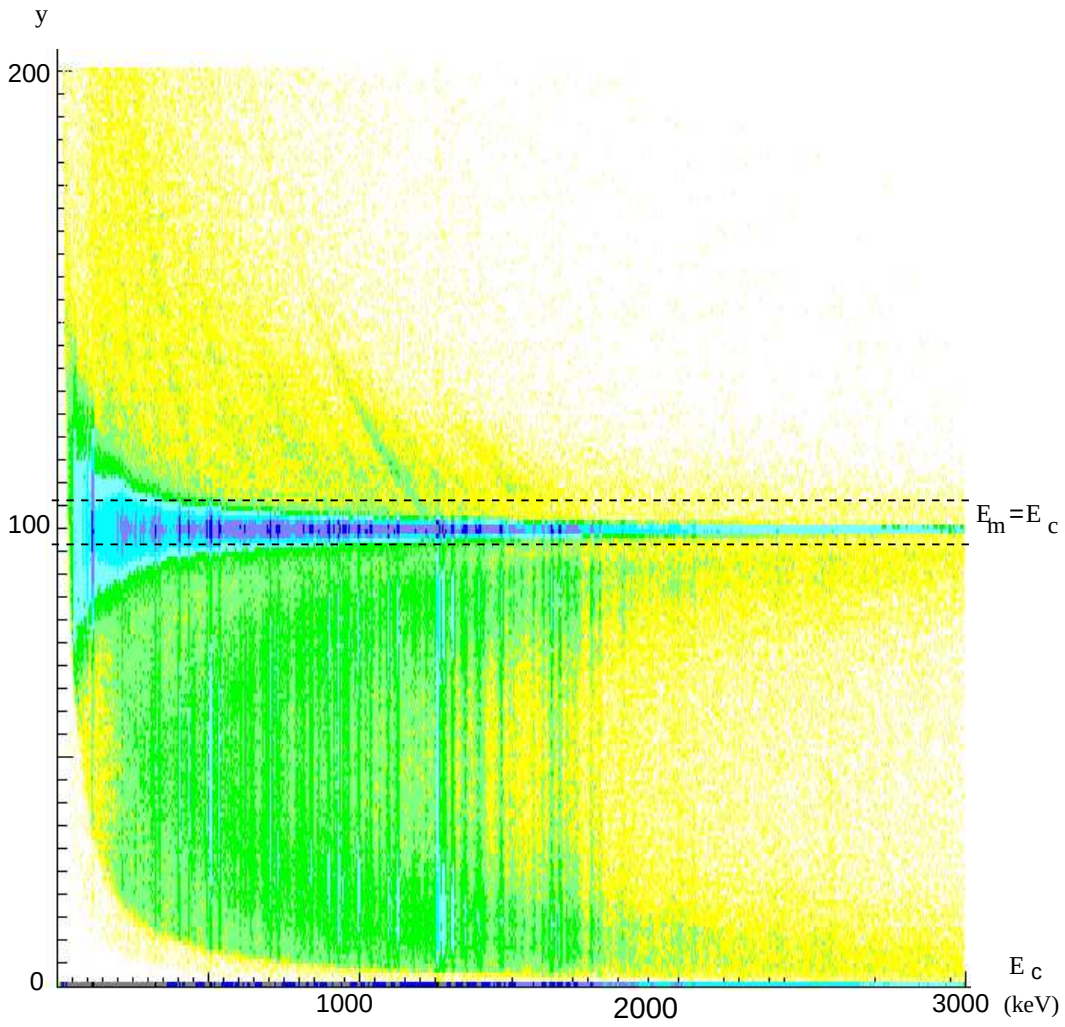

Figure 3.7: Parameter y (Eq. 3.3) as a function of the γ-ray energy, E_γ deposited in a crystal.

horizontal hits in the clovers increase the statistics by ∼25% with respect to the single hits. And yet the FWHM only increased by ∼ 0.2%!

- **Individual velocity correction**

  The last Doppler correction stems from the fact that the recoiling nuclei from different events do not have exactly the same velocity. Their velocity depends on their total kinetic energy, which is measured in the IC. A matrix showing the total energy deposited in the ion chambers right and left side, versus the γ-ray energy was created. With this matrix, we did much like what we did for the angle correction. We sliced the matrix at different IC energy bins and projected the respective γ-ray spectra out. The displacement of a reference peak was measured, and by knowing which slice it is, the velocity correction in known. The correction was put in the program, so that every recoil has a velocity correction depending on their total energy deposited in the IC. The velocity spread in the recoils is ranging from ∼4.0% to ∼4.4% of the speed of

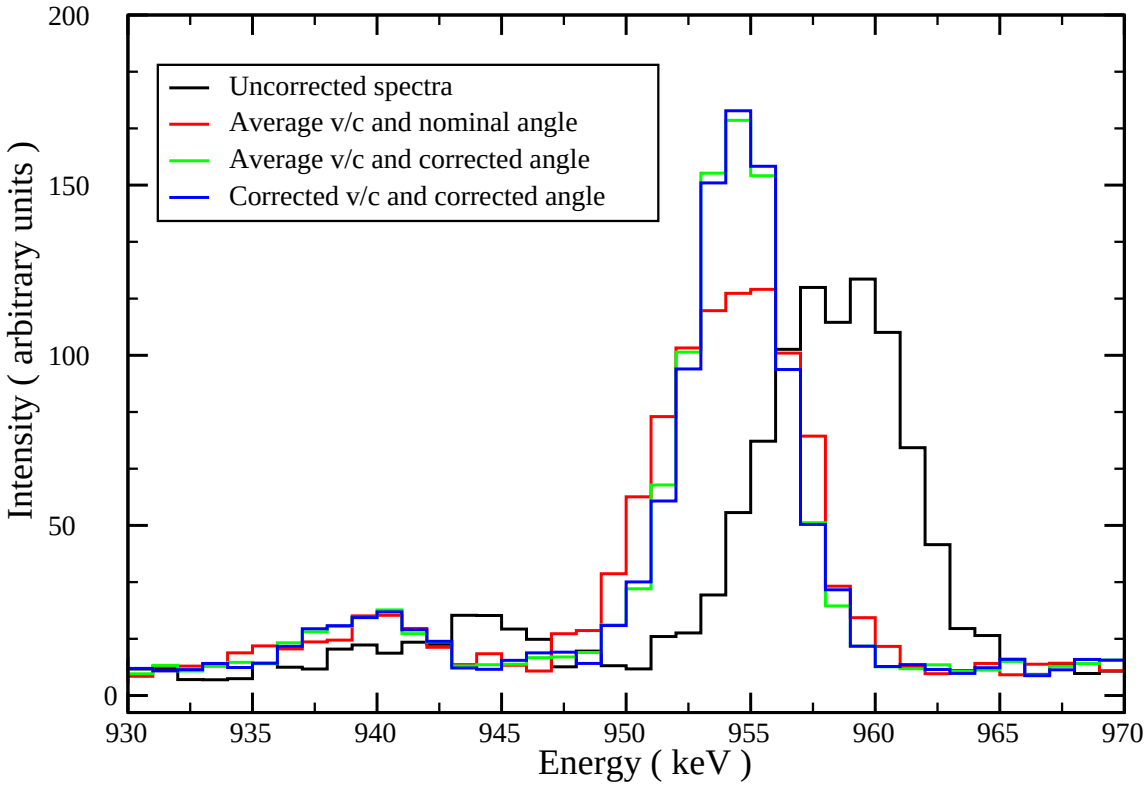

Figure 3.8: A spectra of the effect of the Doppler corrections for a detector placed at 84°.

light. The effect of this correction can be seen in Figs. 3.8 and 3.6. The effect is more prominent for crystals placed at higher angles. The reason for this is again the angular dependence of the Doppler equation 3.1.

This concludes the calibration and corrections for the germanium crystals. The result is higher statistics and narrower peaks, i.e better spectra.

3.3 Calibration of the Recoil Mass Spectrometer and Ion Chamber

The RMS was calibrated to allow the desired A/Q ratio to enter into the IC by setting the values of the magnetic and electric field of the RMS via a computer controlled panel. The energy losses in the three different parts of the ion chamber were made independent of the total energy deposited in ion chamber by the recoiling nuclei. By trying different combinations of the energy losses in the IC, the recoils may be identified by their mass, A, and proton number, Z. Further details on how the calibration of the RMS and IC was done can be found in the Master thesis of Lise-Lotte Andersson [10].
The final sorting of the data was to align all the runs for the two weeks of the experiment. The energy, time, and ion chamber signals were made to overlap for all the

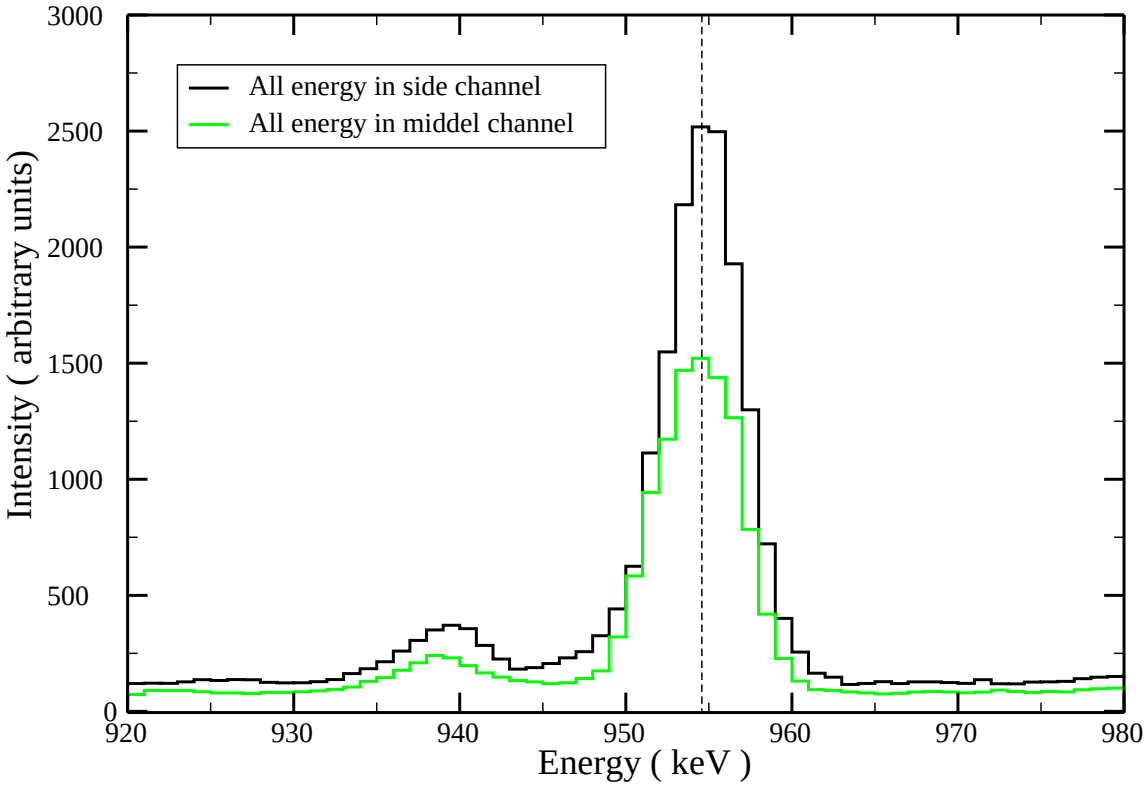

Figure 3.9: Spectra of the very slight difference in the position of the peaks giving rise to the corrected angle, for a detector placed at 84°. The black (green) curve represent the case when the γ-ray has deposited all of its energy in the side channel (middle channel).

runs. This corrects for individual crystals drifting, and changes in the experimental settings during the experiment. The data was then ready to be analyzed.

Chapter 4

Data Analysis

In this chapter a description of how the nuclei were identified, how their spectra were produced, and the following investigation of them is addressed.

4.1 The Recoil-γ Matrix

To identify the excited states in nuclei present in the ion chamber a recoil-γ matrix was created. By gating on known γ-ray transitions in ^{62}Zn (954 keV) and in ^{62}Ga (246keV, 376keV, and 571 keV), different combinations of the energy losses of the nuclei in the three sections of the ion chamber may be tried. Through this an optimum Z resolution for the recoils was searched for. The traditional way of obtaining the Z resolution is taking the sum of the energy loss in part 1 plus the energy loss in part 2, $E_1 + E_2$, modified such that the sum is independent of the total energy loss, $E_{tot} = E_1 + E_2 + E_3$. For mass $A = 62$, however, the energy loss in part 3 minus the energy loss in part 1, $E_3 - E_1$, made independent of E_{tot} gave the best Z-resolution. This will be referred to as the energy loss function (ELF) and the detailed procedure is described in Ref. [10]. The ELF as a function of γ-ray energies was created. This is the recoil-γ matrix for $A = 62$. The matrix is shown in Fig. 4.1, and the positions of ^{62}Ga and ^{62}Zn are indicated. The Z-resolution can be seen in Fig. 4.2. Notice the great difference in abundance of the nuclei. ^{62}Ga is much less common than ^{62}Zn which, of course, is a result of the rarity of neutron evaporation (see Sec. 2.1). As was mentioned before these nuclei are produced in the same reaction, but in different reaction channels. Thus considering the relative statistics of ^{62}Zn and ^{62}Ga, the rarity of ^{62}Ge may be imagined by looking at Fig. 4.2. In Fig. 4.3 the normalized intensities are shown, along with their peak position. The two nuclei have their peaks at different positions along the ELF axis. The figure of merit for the separation of the peaks is;

$$R = \frac{d}{FWHM} = \frac{200 - 175}{230 - 175} \sim 0.45$$

where d is the distance between the peaks and FWHM is the Full Width at Half Maximum of the ^{62}Zn curve.
The ^{62}Zn has 30 protons and peaks at channel 200 in the ELF. ^{62}Ga has 31 protons and peaks at channel 175. Considering this, the assumption that ^{62}Ge with 32 protons should peak at the position of 150 is reasonable. With the present energy

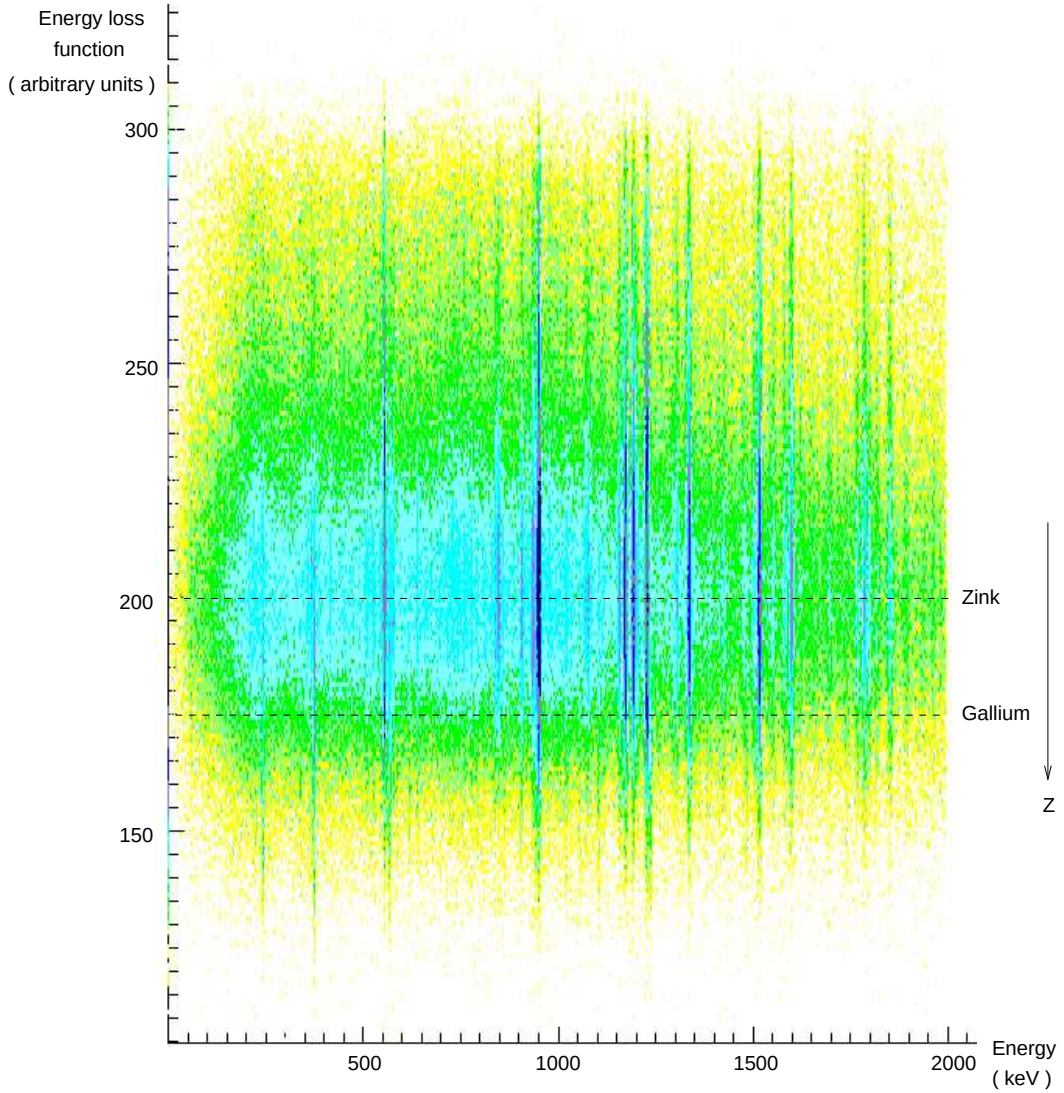

Figure 4.1: The recoil-γ matrix. The positions of ^{62}Ga and ^{62}Zn are marked in the matrix.

loss function, the proton number increases as the ELF decreases. By gating along different intervals on the ELF axis in the recoil-γ matrix and projecting onto the x-axis, the γ-ray spectra of the different nuclei can be produced.

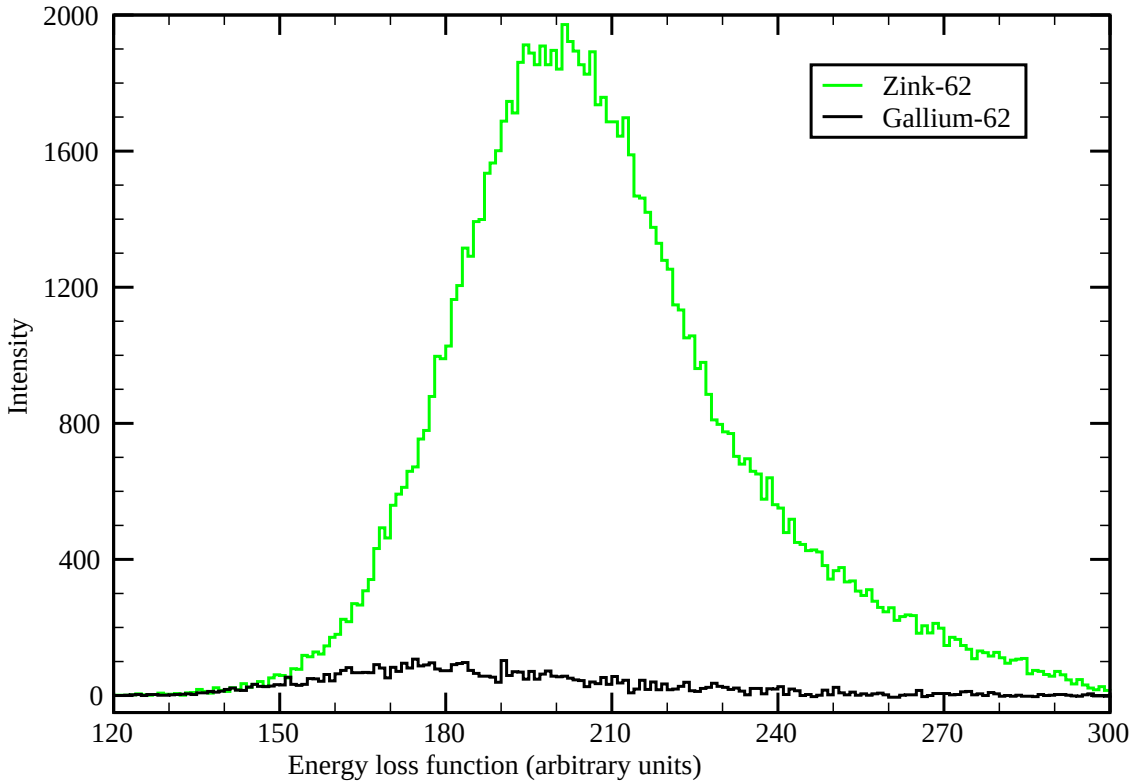

Figure 4.2: The best possible Z-resolution for $A = 62$.

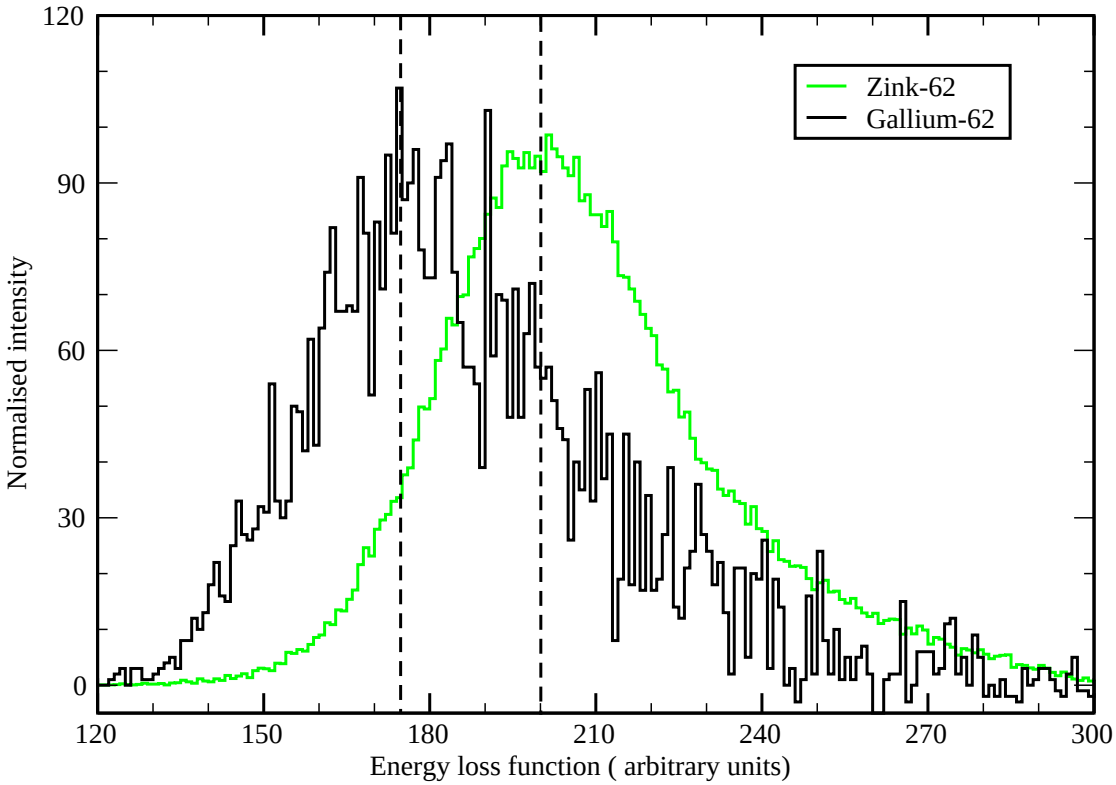

Figure 4.3: The normalized energy loss function curves of ^{62}Ga and ^{62}Zn. ^{62}Ga and ^{62}Zn peak at the channels 175 and 200, respectively. ^{62}Ge is thus expected to peak at channel 150.

4.1.1 Creation of Spectra

The γ-ray spectra produced by gating on different energy loss intervals in the recoil-γ matrix are shown in Fig. 4.4. They are not pure spectra of ^{62}Ga or ^{62}Zn, even though they are created their corresponding intervals in the recoil-γ matrix. The reason for this is, that the gate around the maximum of ^{62}Ga will be "contaminated" by ^{62}Zn (see Fig. 4.2). Thus the spectra are a mixture of both nuclei. Nevertheless the spectra can be cleaned. To clean the spectrum of ^{62}Ga from ^{62}Zn, the following

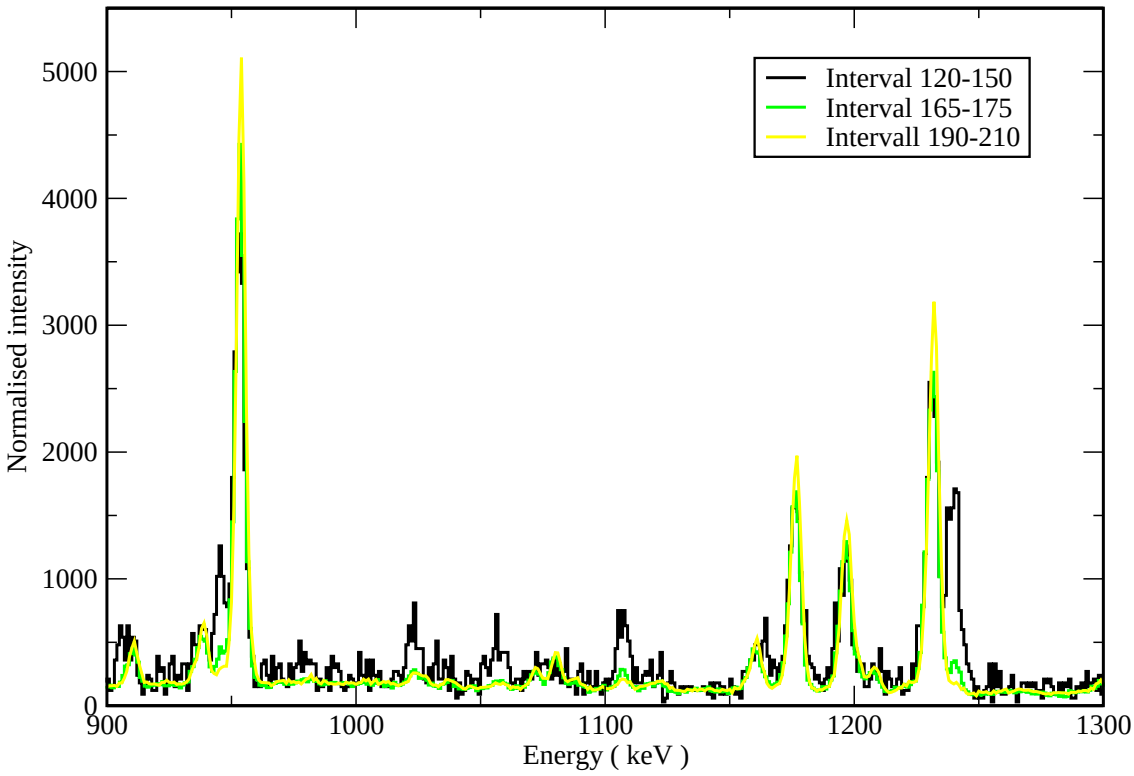

Figure 4.4: Normalised spectra produced by putting gates along the energy loss function in the recoil-γ matrix. The black curve is the interval 120-150, which should contain ^{62}Ge, the green curve is the 165-185 interval, corresponding to ^{62}Ga and the yellow curve(190-210) describes ^{62}Zn. Notice the different mixture of all the nuclei in all spectra.

method was used: The ^{62}Zn spectrum was multiplied with a coefficient to match its peak intensities in the ^{62}Ga spectrum and subtracted from the ^{62}Ga spectrum. By adjusting the coefficients and slightly shifting the position of the ^{62}Zn spectrum, a clean spectrum of ^{62}Ga was achieved. The same method was applied to obtain the clean ^{62}Zn spectrum. The cleaned spectra can be seen in Figs. 4.5 and 4.6. In them some peaks are marked with their energies in keV. A few of the peaks in ^{62}Zn will be discussed in Sec. 5 in relation to a shell-model calculation.

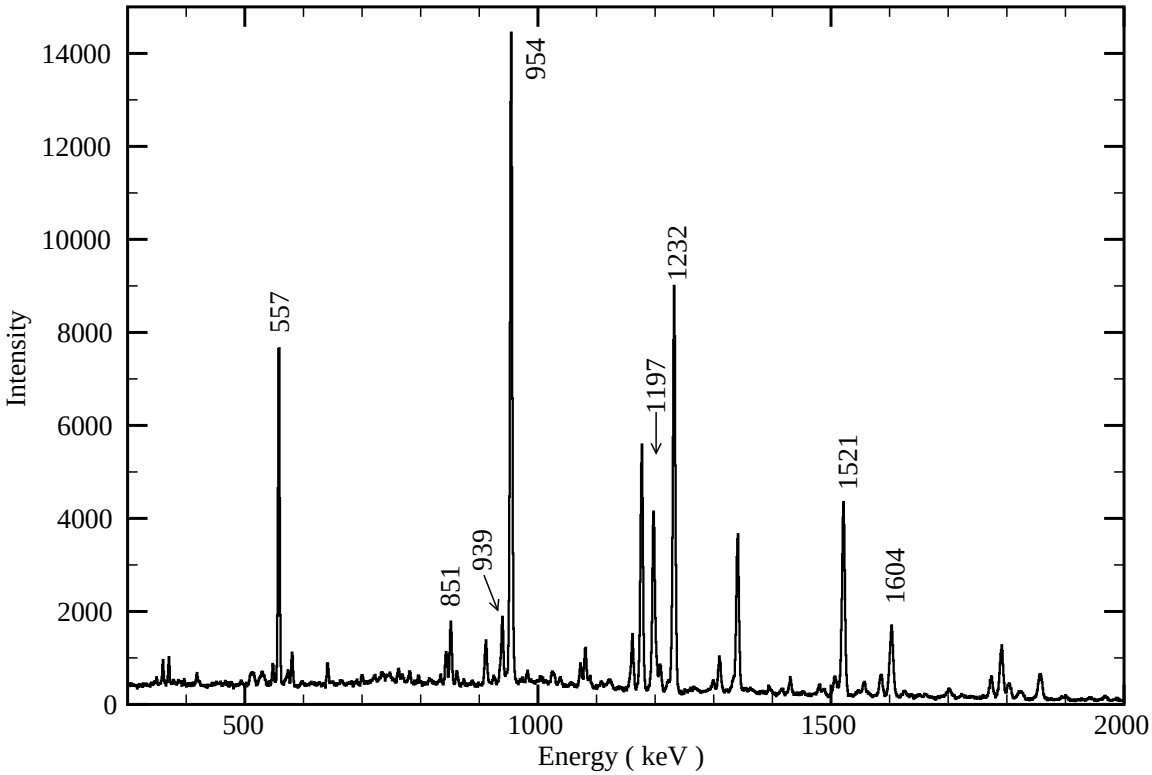

Figure 4.5: The cleaned spectrum of ^{62}Zn. See text for details.

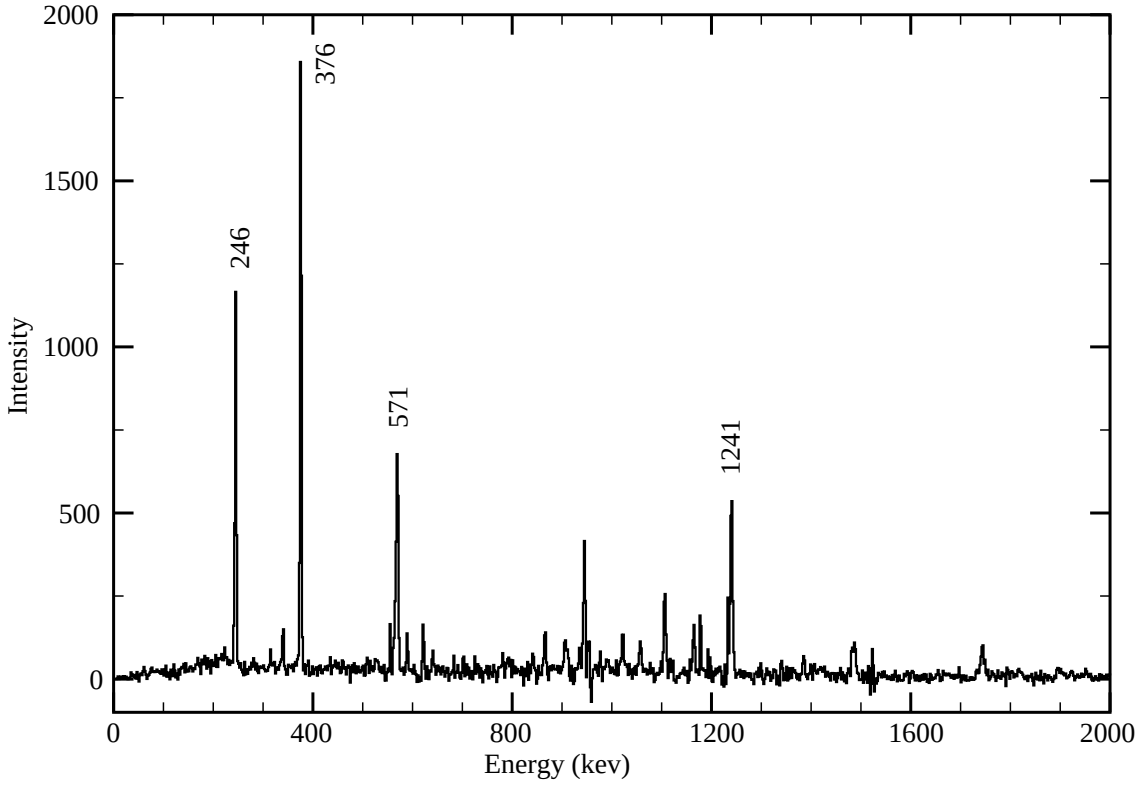

Figure 4.6: The cleaned spectrum of ^{62}Ga. See text for details.

4.2 Investigating the Candidates

A peak belonging to ^{62}Ge should be visible in the γ-ray spectrum gated by the interval 120-150 of the ELF, but as may be seen in Fig. 4.4 there are no striking unknown peaks present. So it can be worth considering a theoretical aspect. As previously mentioned, the mirror nucleus of $^{62}_{32}$Ge is $^{62}_{30}$Zn. ^{62}Ge is then expected to have approximately the same energy in its $2^+ \rightarrow 0^+$ transition as ^{62}Zn. With this in mind a closer look at the energy region around the 954 keV transition in ^{62}Zn was taken. In Fig. 4.7 the spectra produced from the recoil-γ matrix intervals may be seen with some structures marked. Since the structures present in Fig. 4.7 are very weak, the methods of investigating them are limited. I started by looking at

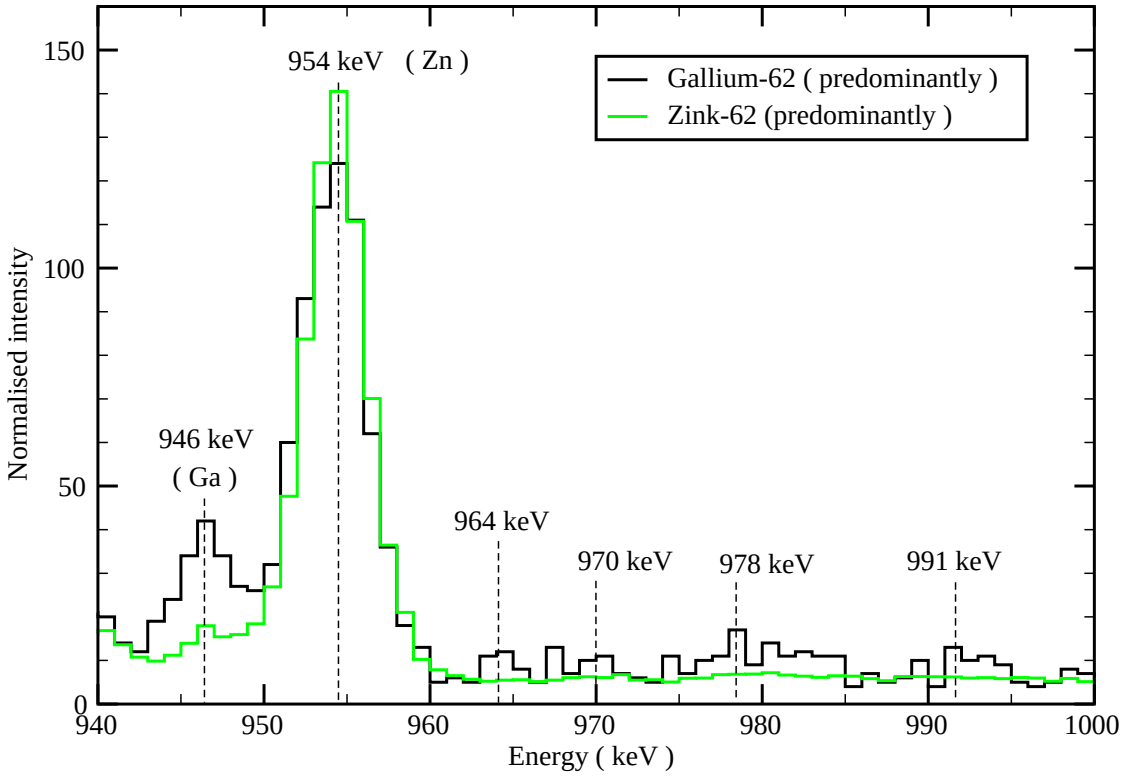

Figure 4.7: Spectra obtained from the recoil-γ matrix, using the intervals 120-150 and 170-179 respectively. The black spectrum shows peaks of mostly ^{62}Ga and ^{62}Ge. The green spectrum contains more ^{62}Zn. The peaks at 946 keV and 954 keV belong to ^{62}Ga and ^{62}Zn respectively. The other structures marked are unknown.

the different structures in a program called `tv` [15]. An average background level in the spectrum corresponding to the ELF interval 120-150 was chosen. The structures were marked and integrated, while the program subtracts the background and gives the peak volume in the marked region. The ELF was scanned from 120 to 210, and the behavior of the different candidates was registered. The result is illustrated in Fig. 4.8. Only one of the candidates stand out from the rest, namely the 964 keV candidate. It has a lokal maximum close to channel 150 in the ELF, which is expected for a transition in ^{62}Ge. The other structures have no peak at 150, though

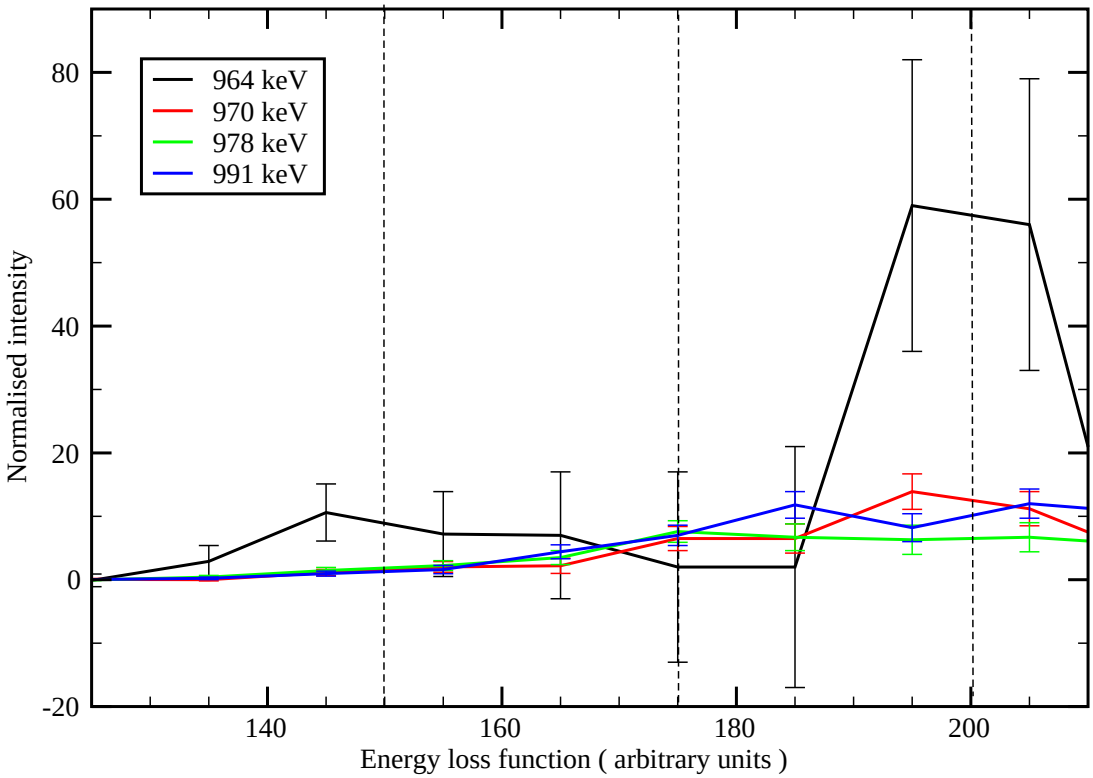

Figure 4.8: The behavior of different candidates to being ^{62}Ge. Only one of the candidates peaks around 150, which is the position where it is expected to find ^{62}Ge.

they all increase in the region around channel 200. This is due to a generally higher background level in the spectra. The 964 keV behavior was also compared with the ground state transitions of ^{62}Ga and ^{62}Zn, namely the 571 and 954 keV peaks in order to check that their behavior does not produce an artificial rise at channel 150 in the ELF. As can be seen in Fig. 4.9 this is not the case. The figure also shows the sensitivity of the 964 keV peak to the background level chosen. With a high background level, the peak almost disappears, which is a result of the poor statistics in the 964 keV peak.

Mirror symmetry arguments also predict a peak in the energy region of 1200-1300 keV. This area was investigated in the same way as described above. In Fig. 4.10 the spectra of the different intervals from the recoil-γ matrix are shown, again with some structures marked out. The behavior of these structures as the energy loss function is scanned is shown in Fig. 4.11. Again, only one peak displays a different behavior. The 1321 keV peak has a slight maximum in the region corresponding to ^{62}Ge. This is the second candidate to being a transition in ^{62}Ge. However, it is a much less reliable than the 964 keV peak, since the 1321 keV peak is weaker, and its maximum in the ELF plot is not so pronounced. The 964 keV and 1321 keV peaks are the only candidates to being γ-ray transitions from the excited ^{62}Ge nuclei, which were possible to identify.

Since the statistics in the peaks is so small, I wanted to rule out that these energies

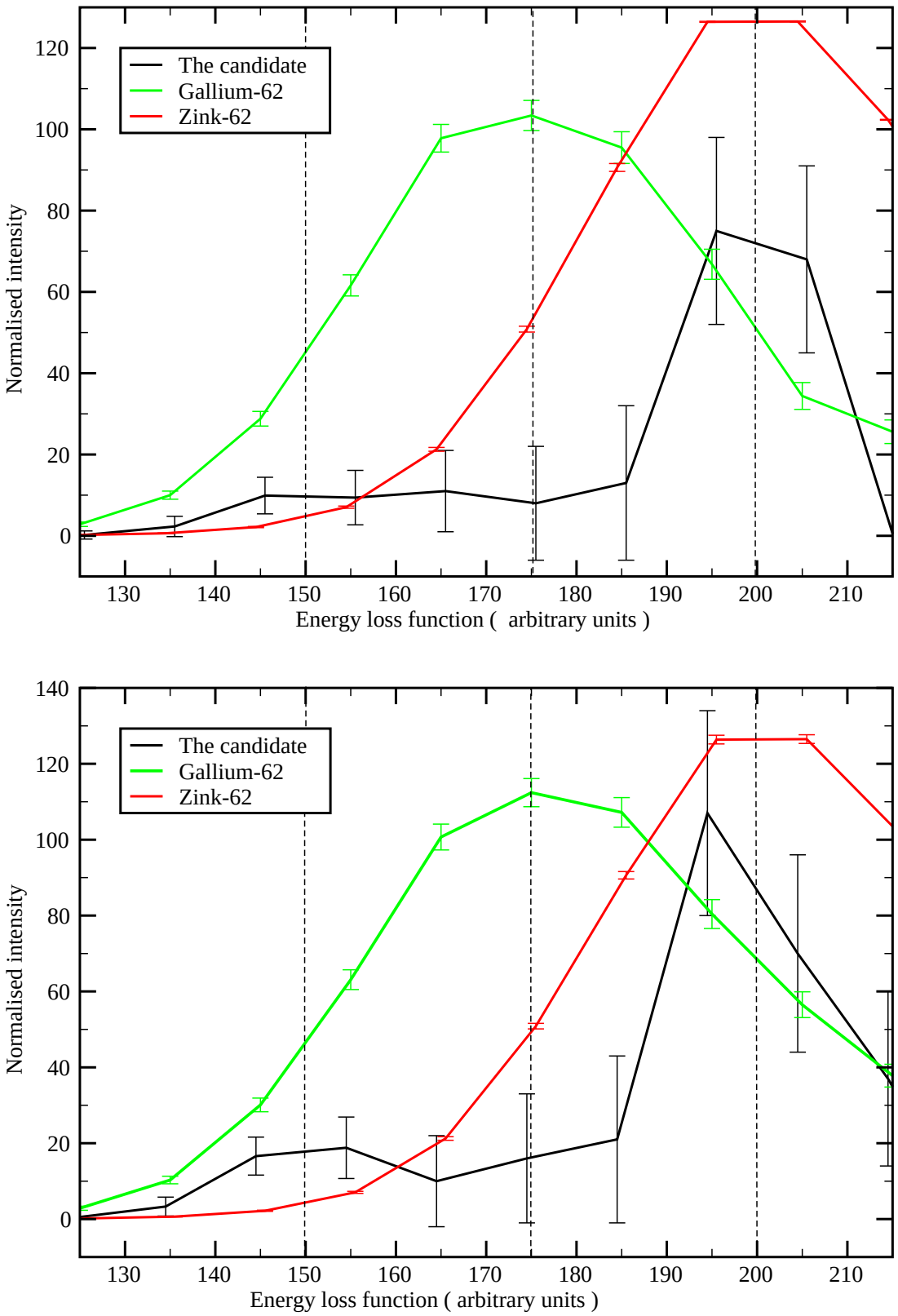

Figure 4.9: The behavior of the strongest candidate for ^{62}Ge.Top: high background level. Bottom: average background level. The curves of the ground state transitions in ^{62}Ga and ^{62}Zn are included for reference. The dotted vertical lines show where ^{62}Ge, ^{62}Ga, and ^{62}Zn should be the strongest.

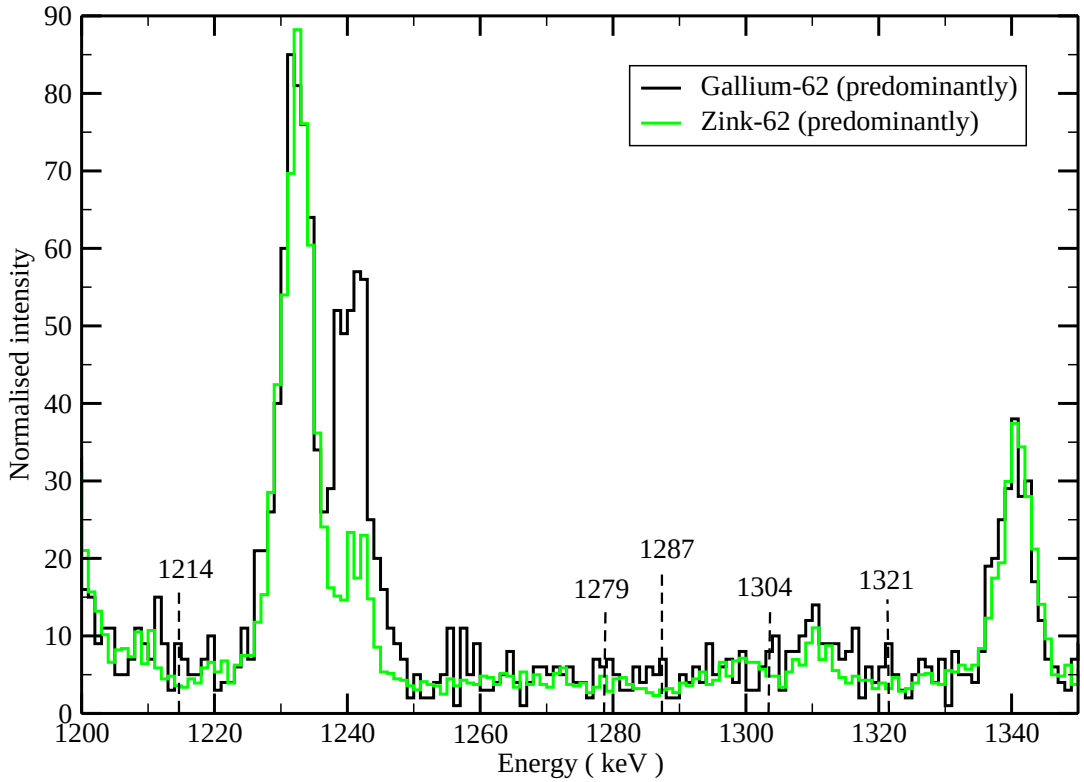

Figure 4.10: Same as Fig. 4.7 but for a different γ-ray energy range.

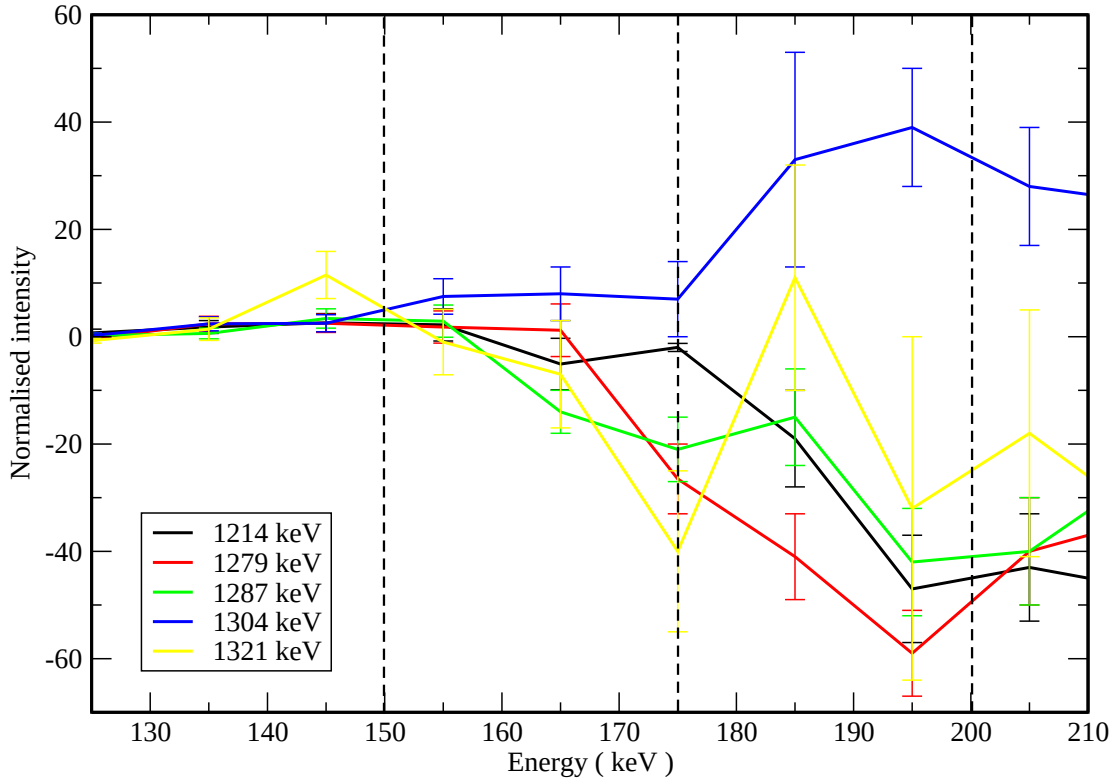

Figure 4.11: Same as Fig. 4.9, for an average background level.

could belong to any known isotopes. Maybe the γ-ray energies could come from some contamination in the target or the target chamber. In our experiment reaction products with masses between A$\simeq$45 to A=62 can be created via reactions on the ^{24}Mg target or carbon and oxygen contaminations on it. A current database was scanned for the 964 keV and 1321 keV γ-ray energies. For the 964 keV candidate, the same γ-ray energy is known in ^{48}Ca, ^{49}Ti, ^{54}Co, ^{60}Co, and ^{61}Cu. Out of these it is only possible to have ^{60}Co and ^{61}Cu in the ion chamber. ^{61}Cu is produced in the strong reaction channel of 3p, is it possible to have it in random coincidence in the ion chamber? If the 964 keV transition here corresponds to a transition in ^{61}Cu then other transitions from ^{61}Cu must also be present. An investigation of the spectra shows no other ^{61}Cu transitions. Hence the 964 keV peak does not belong to ^{61}Cu. ^{60}Co may be produced with the ^{25}Mg contamination in the target, but in order to reach ^{60}Co five protons have to be evaporated, and with the energy of this experiment this is not possible. And no other peaks from ^{60}Co is present in the spectra. The same kind of investigation was performed for the 1321 keV peak, with a similar result. Thus it is found that the γ-rays cannot come from other possible nuclei, making it more probable that they do belong to ^{62}Ge.

Chapter 5

Discussion on the Candidates

To investigate the atomic nucleus from a theoretical point, it is necessary to solve the Schrödinger equation, HΨ=EΨ. The solution contains among other things information on the energy levels. The Hamiltonian describes the total energy in the system. For a nucleus it is:

$$H = \sum_{i=1}^{A} \left(-\frac{\hbar^2}{2m} \nabla_i^2 \right) + \frac{1}{2} \sum_{i \neq j}^{A} v(\vec{r}_i, \vec{r}_j) \tag{5.1}$$

The first part of Eq. 5.1 describes the kinetic energy of the system, and the second part describes the interaction of the nucleons with each other. However, the interaction between the nucleons is not fully understood, but for a given nucleon the interaction term is an average potential generated by all the other nucleons. Often a Woods-Saxon potential (Eq. 5.2) to which different terms may be added to better reproduce the experimental data, is used to approximate the interaction.

$$V_{eff}(r) = \frac{-V_0}{1 + e^{\frac{r-R}{a}}} \tag{5.2}$$

where the well depth V_0 is of the order of 50 MeV, R is the nuclear radius given by $R = R_0 A^{1/3}$ fm ($R_0 \approx 1.25$ fm), and A is the mass number of the nucleus. The skin diffuseness is represented by the parameter a, which is approximately 0.55 fm. Often a spin-orbit interaction is added to the Woods-Saxon potential. The Hamiltonian then reproduces the experimentally observed level structures of nuclei generally well. The nucleus may be described as having a shell structure, in close analogy with the shell structure of atomic electrons. A shell can be thought of as several close lying energy levels, with energy gaps above and below it. A closed shell is very stable due to the large energy difference to other levels. The so called magic numbers indicate the closure of major shells, these are for both protons and neutrons N,Z=2, 8, 20, 28, 50, and 82.

The ground state configuration of ^{62}Ge is indicated in Fig. 5.1. The shells are completely filled up to the $1f_{7/2}$ shell for both protons and neutrons. The next shell, the $2p_{3/2}$ shell is filled for protons, but not for neutrons. The ground state of even-even nuclei like ^{62}Ge is 0^+. This depends on the residual pairing force, which tends to couple two like particles to spin zero. In Fig. 5.1 the ground state configuration of ^{62}Zn is also present, since it is the mirror nucleus of ^{62}Ge. As was mentioned

in the introduction, mirror nuclei are expected to have similar level structures. If the strong force is charge independent the differences in level structures of mirror nuclei should only depend on the Coulomb force. By studying mirror nuclei a better understanding of which configuration of nucleons forms an excited state may be achieved.

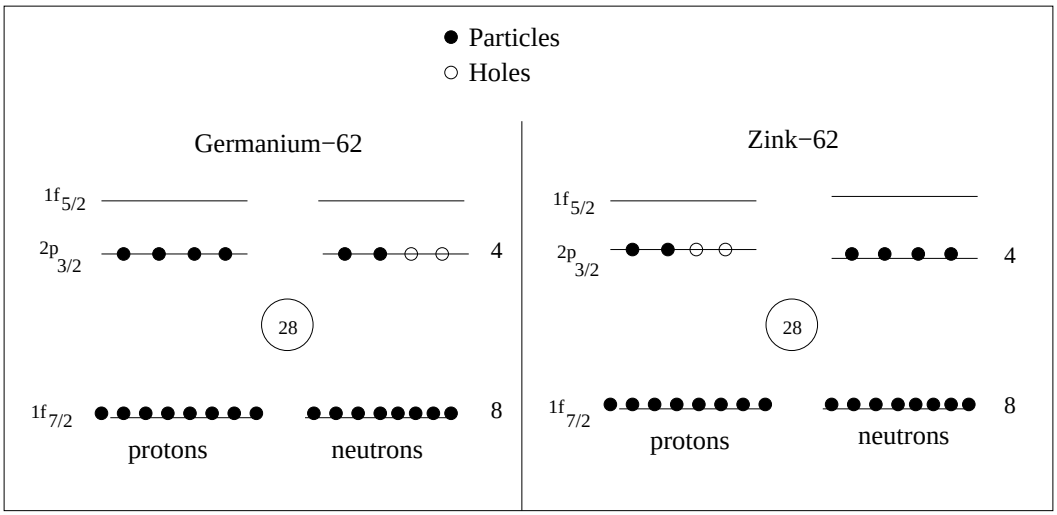

Figure 5.1: The ground state shell structure of ^{62}Ge and ^{62}Zn. The filled (empty) circles represent particles (holes). The notation of the shells in the figure are nl_j. n is the number of shells with the same l value, l is the orbital angular momentum, and $j = s + l$. The numbers on the right hand side correspond to the maximum number of protons and neutrons allowed in each sub shell. The number inside the circle is the magic number of 28. It indicates a major shell closure.

If the charge of the proton is disregarded, then protons and neutrons are expected to be very similar. A quantum number describing the protons and neutrons as being the same particle but in different states, may be introduced. It is called the isospin quantum number, t. The neutron has an isospin projection of $t_z = +1/2$ and the proton has $t_z = -1/2$. The total isopsin of a nucleus is $T_z = \frac{1}{2}(N - Z)$. Thus ^{62}Ge has T_z=-1 and ^{62}Zn has T_z=+1. Almost all known even-even nuclei have their first two excited levels as 2^+ and 4^+. The 964 keV and 1321 keV γ-rays found in the experiment are therefore believed to correspond to the first two yrast states of ^{62}Ge, which is shown in Fig. 5.2 along with the relevant part of the level scheme of ^{62}Zn. From Fig. 5.2 it can be seen that the decay energies of ^{62}Zn and ^{62}Ge are indeed similar.

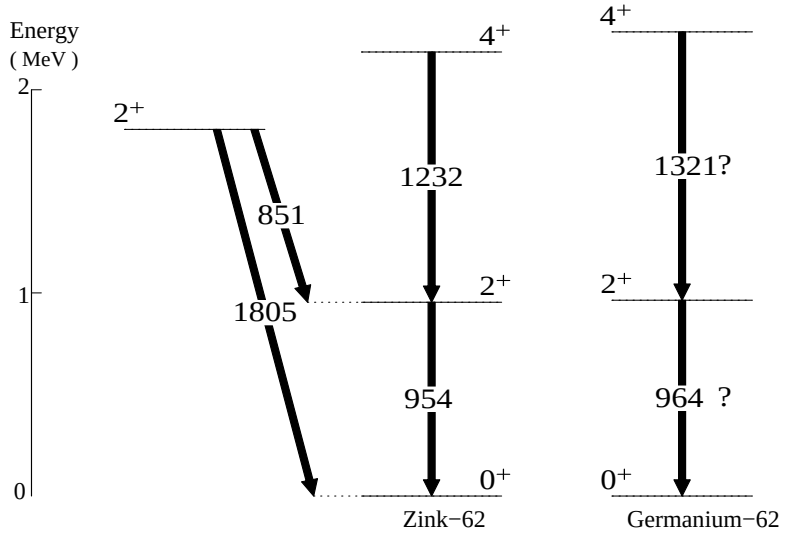

Figure 5.2: The lowest lying transitions in ^{62}Zn (some of these transitions are marked in Fig. 4.5) and the possible level scheme of ^{62}Ge.

To further compare the experimental results, a shell-model calculation was performed, using the code `Antoine` [12, 13] and the KB3G interaction with Coulomb matrix elements [14]. The calculation was performed in the fp model space allowing for three particles to be excited between $1f_{7/2}$ shell and the upper fp shell. The two first excited levels were calculated with two different assumptions:

1. The first calculation assumed that the energy needed to excite a nucleon to the next level is the same for both protons and neutrons, so called Same Single Particle energy (SSP).

2. The second calculation assumed that the energy needed to excite a nucleon to the next level depends on if it is a proton or a neutron, so called Different Single Particle energy (DSP).

The result of the calculation is summarized in Table 5.1. The calculated values in Table 5.1 do not correspond to the measured energies very well, even for ^{62}Zn. With a shell-model calculation it is hard to reproduce the experimental values in this mass region. This is mainly due to the many different possible ways of excited configurations and how many particles which are allowed to participate in them. In particular the influence of the l=4, $g_{9/2}$ shell is a question of ongoing theoretical efforts. Setting these problems aside one can notice that the calculated energy levels of ^{62}Ge are higher than the calculated energy levels for ^{62}Zn, which does reflect the experimental results. So the relative energy levels of the nuclei are more easily reproduced for the shell-model calculation than the absolute values.
The probabilities for different excited configurations was also calculated with the above mentioned shell-model calculation. It turns out that the 2^+ is formed by

	^{62}Ge			^{62}Zn		
Level	E_{EXP}	E_{SSP}	E_{DSP}	E_{EXP}	E_{SSP}	E_{DSP}
2^+	964	1215	1221	954	1187	1184
4^+	2285	2679	2798	2186	2703	2700

Table 5.1: The calculated excitation energies for ^{62}Ge and ^{62}Zn using the code `Antoine` and the experimental values. See text for details.

aligning the two neutrons in the $2p_{3/2}$ shell, which is not very surprising. The 4^+ state, however, is formed by breaking a proton pair, and exciting one of the protons into the $1f_{5/2}$ shell. This is surprising considering that the protons form a closed $2p_{3/2}$ shell.
The excitation energy difference between corresponding levels of the mirror nuclei is called the Mirror Energy Difference (MED). It is defined as:

$$MED = E(T_z = -1) - E(T_z = 1)$$

The MED as a function of spin can provide useful information. Fig. 5.3 displays the experimental and the calculated MED. The experimental and DSP calculated points do show a similar behavior, even though their values do not perfectly match. The aligning of neutrons to form the 2^+ state is the better described by the SSP calculation than the DSP calculation, as can be seen in Fig 5.3. This depends on the fact that to align the neutrons it is not necessary to cross into another shell. The 4^+ state is better described by the DSP calculation, which is expected since a nucleon pair is broken and one nucleon is excited into the $1f_{5/2}$ shell. For the 4^+ state the SSP calculation does not work at all. This implies that indeed the energy level difference between shells is different for protons and neutrons. This can depend on a lot of things. When the proton is excited into a new shell, the charge distribution of the nucleus changes. For the shells in question here it means that their energy levels are repelled from each other. Another effect is the spin-orbit effect. Nuclei in this mass region are also known to rapidly change their shape with the excitation energy, which may also influence the energy levels. So the energy distance between the levels is different for protons and neutrons, i.e, for ^{62}Ge and ^{62}Zn. When the proton pair in ^{62}Ge is broken to form the 4^+ state, the average distance between the protons increases. This reduces the Coulomb repulsion between them, as the repulsion is inversely proportional to the distance between them. The reduction in Coulomb repulsion leads to higher binding energies. For neutrons this effect does not exist, as the neutron is uncharged. It is thus expected that the MED should increase with increasing spin, which is indeed what is seen in Fig. 5.3.
The calculated probability to form the 4^+ state by breaking the neutron pair in ^{62}Ge is less than 1% of all the different possibilities. Why does the nucleus prefer to excite protons rater than neutrons, even though the protons form a full shell in $2p_{3/2}$? It may depend on that if the protons are excited, the binding energy increases and the nucleus achieves an as proton deficient core as possible. To be able to determine with more certainty which configuration that forms an excited state, more experimental

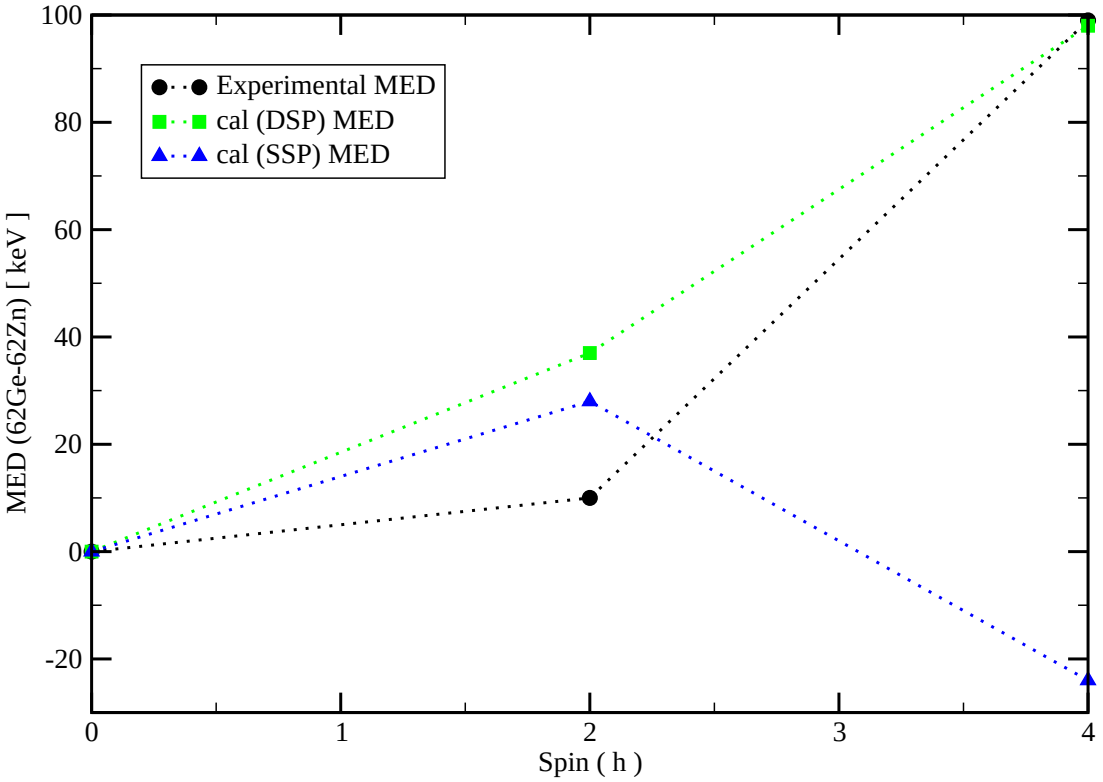

Figure 5.3: The calculated and experimental Mirror Energy Difference (MED) of ^{62}Ge and ^{62}Zn. See text for details.

data is needed. There is also the question of how reliable the shell-model calculation is in this mass region. Nevertheless, the two γ-ray energies can be understood and explained from basic theoretical arguments.

Chapter 6

Conclusions and Outlook

From the analysis of the present experiment two tentative γ-ray transitions in ^{62}Ge were found. As mentioned in Sec. 1, the problems with the experimental equipment, first of all the ion source, led to the loss of almost half of the originally expected statistics. This unfortunately implies that it is not possible to prove that these γ-rays definitely belong to ^{62}Ge. However, indirect evidence can be provided:

- The 964 keV and 1321 keV γ-ray energies are from an $A = 62$ nucleus and likely $Z = 32$, as indicated by their ELF plots.
- The two γ-ray transitions cannot be associated to any kind of background or contamination radiation from nuclei with $45 \leq A \leq 62$.
- They follow the basic theoretical expectations of mirror nuclei.
- The MED diagram shows a similarity between the experimental points and the points calculated with contemporary large scale shell-model calculations.

Nevertheless, the only way to truly prove that these γ-ray energies belong to ^{62}Ge is through new experiments. During spring 2004 two new experiments are envisaged, which are expected to provide more information on ^{62}Ge. A follow-up experiment at Oak Ridge National Laboratory is planned, which will be performed under the same conditions as the first experiment. Hopefully, the contributed statistics from the old and new experiment will be enough to establish the excited levels of ^{62}Ge. The other experiment is to be conducted at the Argonne National Laboratory, with the same fusion-evaporation reaction as in Oak Ridge, but with a higher beam energy. It is expected, even with the higher beam energy that ^{62}Ge may be found anyway, due to the very long beam time (10 days) allocated for us there.
The relative cross section of ^{62}Ge was estimated before the experiment was performed. It is now interesting, especially considering the new experiments, to find an experimental cross section for ^{62}Ge. The relative intensities of the ground state transitions in ^{62}Zn, ^{62}Ga, and ^{62}Ge were determined with the program `eff_rib096_all`. It converted the measured peak intensities in the spectra produced from the entire recoil-γ matrix, into relative intensities. The result can be seen in Table 6.1. For every produced ^{62}Ge nucleus, 5000 ^{62}Zn nuclei are produced. This is very interesting since it corresponds exactly to the anticipated cross section of ^{62}Ge before the experiment. First of all, this is yet another reason to believe that the transitions

Nucleus	Relative intensity	Relative production cross section
^{62}Zn	103 ±4	5000
^{62}Ga	15 ±1	750
^{62}Ge	0.02 ±0.01	1

Table 6.1: The relative intensities calculated using the code `eff_rib096_all` and the approximated relative production cross section.

of interest belong to ^{62}Ge. Secondly, it is good since the new experiment can be performed with the same conditions as the first experiment.
There are ongoing efforts in the nuclear structure group in Lund to study mirror nuclei. They are focusing on the finer details associated with different effects of the Coulomb force and possible indications for the strong force not being charge independent [16]. When the excited levels of ^{62}Ge have been firmly established, they will contribute to the understanding of even-even nuclei far from stability. Hopefully this may lead to further improvements on the shell model parametrisation just above ^{56}Ni -in particular, the development of a reliable fp $g_{9/2}$-shell-model space ,which can reveal insights on how the forces work inside the atomic nucleus.

Acknowledgements

I would like to thank Prof. Claes Fahlander for introducing me to the field of nuclear structure physics in the first place, and for allowing me to participate in the experiment. It was very interesting and I got to experience that 'beam time feeling'.
I am very grateful for the patient guidance and help from my excellent supervisor, Dr. Dirk Rudolph. But most of all I am thankful to you for inspiring me to learn so much more physics.
I would also like to thank Jörgen Ekman for his help, but in particular for performing the shell-model calculation and Rickard Du Rietz, for managing all of my computer catastrophes. I am also obliged to Lise-Lotte Andersson for making every day at the office enjoyable.
A general thanks goes out to all the members of the nuclear structure group for providing a very pleasant atmosphere, both on work related issues and leasure wise.
I would also like to thank the people who helped us with the experiment, the collaborator from Keele university, Gavin Hammond and the people at Oak Ridge national laboratory, especially David Radford and Carl Gross.
The weekly nuclear coffee meetings are also appreciated for broadening my perspective on nuclear structure physics.
Finally, I would like to thank my family and friends for their support and love.

Bibliography

[1] K.S Krane, Introductory Nuclear Physics, Wiley & Sons, New York, (1988).

[2] J. Ekman, Isospin symmetry breaking in the A=51 mirror nuclei, Licentate thesis, Department of Physics, Lund University (2003)

[3] http://www.phy.ornl.gov/hribf/research/equipment/clarion/

[4] C.J Gross *et al.*, Nucl. Instr. Meth. A **450**,12-29 (2000).

[5] C.J Lister, *et al.*, Phys. Rev. C**42**, 1191 (1990).

[6] W. Gellertly, *et al.*, Phys. Lett. B**253**, 287 (1991).

[7] S.M. Fischer, *et al.*, Phys. Rev. Lett. **87**,132501 (2001).

[8] S.M. Fischer, *et al.*, Phys. Rev. Lett. **84**, 4064 (2000).

[9] G.F Knoll, Radiation Detection and Measurement, 3rd edition, Wiley

[10] L-L Andersson, Master thesis, Lund University, LUNFD6/ (NFFR-5022)1-47/(2004)

[11] D.C. Radford, Radware γ-analysis software package.

[12] E. Caurier, Fres, Strasbourg, 1989-2002

[13] E.Caurier, F.Nowacki,Acta Pysica Polonica 30 (1999) 705

[14] J. Ekman, priv. comm.

[15] J.Theuerkauf, S.Esser, S. Krink, M. Luig, N. Nicolay, O. Stuch, H. Wolters, Program Tv, University of Cologne, unpublished.

[16] J. Ekman, Ph. D. thesis, Lund University, to be published